iScience

CellPress
OPEN ACCESS

Article

Engineering branched ionizable lipid for hepatic delivery of clustered regularly interspaced short palindromic repeat-Cas9 ribonucleoproteins

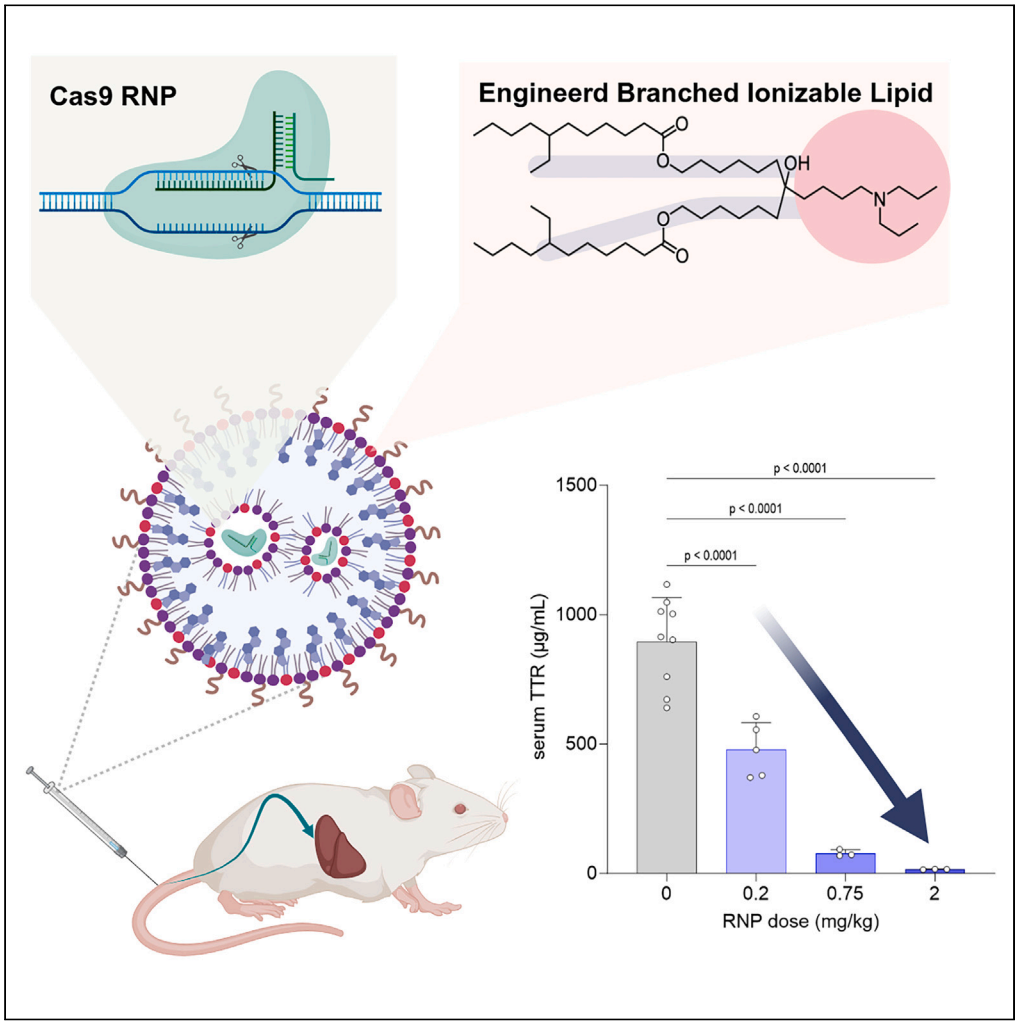

Haruno Onuma, Rina Shimizu, Yuichi Suzuki, Mina Sato, Hideyoshi Harashima, Yusuke Sato

y_sato@pharm.hokudai.ac.jp

Highlights

Structure of ionizable lipid suitable for hepatic delivery of Cas9 RNP is identified

The RNP-loaded LNP achieved over 98% reduction of TTR protein level after a single dose

The best ionizable lipid is biodegradable and provides excellent safety for the LNPs

The finding supports the feasibility of *in vivo* genome editing therapy by RNP delivery

Onuma et al., iScience *27*, 110928
October 18, 2024
https://doi.org/10.1016/j.isci.2024.110928

iScience

CellPress
OPEN ACCESS

Article

Engineering branched ionizable lipid for hepatic delivery of clustered regularly interspaced short palindromic repeat-Cas9 ribonucleoproteins

Haruno Onuma,[1] Rina Shimizu,[1] Yuichi Suzuki,[1] Mina Sato,[2] Hideyoshi Harashima,[2] and Yusuke Sato[1,2,3,*]

SUMMARY

The delivery of the CRISPR/Cas ribonucleoprotein (RNP) has received attention for clinical applications owing to its high efficiency with few off-target effects. Lipid nanoparticles (LNPs) are potential non-viral vectors for the delivery of RNPs. Herein, we report the engineering of a branched scaffold structure of ionizable lipids for the hepatic delivery of RNPs. Both the total carbon number and branching position were critical for the functional delivery of RNPs. The optimal ionizable lipid exhibited a more than 98% reduction in transthyretin protein after a single dose with no obvious signs of toxicity. The mechanistic study has revealed that optimal LNPs have a unique "flower-like structure" that depends on both the lipid structure and the payload and that these LNPs accumulate in hepatocytes in an apolipoprotein E-independent manner. These results represent a major step toward the realization of *in vivo* genome editing therapy via RNP delivery using chemically synthesizable LNP formulations.

INTRODUCTION

The clustered regularly interspaced short palindromic repeat (CRISPR)-associated (Cas) system, discovered in 2012, has attracted a great deal of attention from researchers because of its simplicity of design. This system is currently being investigated in basic research and in a number of therapeutic applications.[1] Most of the current clinical trials of gene editing therapies involve *ex vivo* gene editing by means of electroporation of mRNA encoding the CRISPR/Cas system wherein the therapeutic effect is achieved by transplanting edited cells into patients.[2] The Food and Drug Administration (FDA) approved CASGEVY, the first CRISPR-based *ex vivo* gene-editing therapy for sickle cell disease in 2023. While *ex vivo* gene editing is advantageous in terms of efficacy as well as safety because only precisely edited cells can be selected, expanded, and transplanted into patients, its application is restricted to certain specific cells such as hematopoietic stem cells and T cells. In addition, the preparation of *ex vivo* edited cells is accomplished at a high cost as it requires special techniques and facilities. On the other hand, *in vivo*, gene editing that achieves a therapeutic effect through the direct administration of genome editing tools into patients either locally or systemically is considered a promising therapeutic strategy for the treatment of genetic diseases. Although *in vivo* genome editing is beneficial in terms of simplicity, the development of efficient, specific, and safe vectors and treatment protocols remains challenging.

Lipid nanoparticles (LNPs) are non-viral chemically synthesized vectors that have been widely studied, particularly when used for the delivery of nucleic acids. Rational designs and combinatorial approaches to ionizable lipids have led to drastic improvements in the functional delivery of both short interfering RNA (siRNA) and mRNA *in vivo*,[3] which thus far has resulted in the approval of three LNP-based RNA therapies.[4] In 2021, the first clinical trial of *in vivo* CRISPR/Cas genome editing therapy using an LNP was reported.[5] NTLA-2001, an LNP encapsulating both single-guide RNA (sgRNA) against transthyretin (TTR) and mRNA encoding *Streptococcus pyogenes* Cas9 (spCas9), was examined for the treatment of TTR amyloidosis and achieved an 87% reduction in TTR protein at 0.3 mg/kg in the ongoing phase 1 clinical study. This LNP is currently in phase 3 clinical trials as the first *in vivo* CRISPR-based candidate to begin late-stage clinical development. The same technology was applied to the treatment of hereditary angioedema (HAE) by targeting the KLKB1 gene that encodes the kallikrein B1 protein. This approach achieved a 95% reduction in plasma kallikrein protein at a dose of 75 mg RNA in an ongoing phase 1/2 clinical trial.[6]

There are three modes for delivery using the CRISPR/Cas system: DNA (plasmid RNA or DNA viral vectors), RNA, and RNP.[7] In the case of the delivery as DNA, the durable expression of Cas9 proteins in the cells causes an increase in undesired cleavage and editing in untargeted genomic loci.[8] Many double-strand breaks (DSBs) caused by the durable expression of Cas9 proteins have been reported to cause chromothripsis and activate p53 proteins to induce cancer.[9,10] In addition, double-strand DNA (dsDNA) has the potential to be integrated into the site of DSBs and even in random genomic loci. Furthermore, adeno-associated viral (AAV) vectors, which are widely used for genome editing in both basic research and clinical trials have strong immunogenicity, which limits both the level and the number of dosages.[11] Delivery as RNA is the current standard strategy for *in vivo* genome editing because LNP systems were established for the delivery of RNA. However, the

[1]Laboratory for Molecular Design of Pharmaceutics, Faculty of Pharmaceutical Sciences, Hokkaido University, Kita-12, Nishi-6, Kita-ku, Sapporo 060-0812, Japan
[2]Laboratory of Innovative Nanomedicine, Faculty of Pharmaceutical Sciences, Hokkaido University, Kita-12, Nishi-6, Kita-ku, Sapporo 060-0812, Japan
[3]Lead contact
*Correspondence: y_sato@pharm.hokudai.ac.jp
https://doi.org/10.1016/j.isci.2024.110928

expression of Cas9 protein from mRNA lasts for several days and the formation of RNPs in the complicated and unstable cytosol is not an efficient process,[12] which nonetheless is needed in order to achieve genome editing. Delivery as RNPs, in which an active molecule is formed before being introduced into target cells, can circumvent many of the inefficient intracellular processes that are required for delivery as DNA and RNA. In addition, the transient presence of RNPs in cells limits the number of undesired off-target DSBs. Therefore, delivery as RNPs is a promising approach from aspects of both a high level of efficiency and a low level of off-target effects.

Despite the above-mentioned benefits of RNP delivery, there are many challenges that should be addressed: loading efficiency, delivery efficiency, stability, and toxicity.[13] Wei et al. reported the delivery of RNPs into the liver by LNPs composed of both ionizable lipid 5A2-SC8 and permanent cationic lipid 1,2-dioleoyl-3-trimethylammonium-propane (DOTAP) (5A2-DOT-LNPs).[14] Three intravenous injections of the 5A2-DOT-LNPs targeting proprotein convertase subtilisin/kexin type 9 (Pcsk9) at a dose of 2.5 mg sgRNA/kg achieved an approximately 40% reduction in serum Pcsk9 protein. Lee et al. developed CRISPR-Gold loading of both RNPs and a DNA template for homology-directed DNA repair and successfully restored dystrophin expressions of as much as 6% after intramascular injection at a dose of 6 mg Cas9/kg in mdx mice.[15] Gong et al. developed a liposome-coated mesoporous silica nanoparticle (lipoMSN) loading of Cas9 RNPs and achieved a 50% decrease in serum cholesterol following the administration of lipoMSN targeting both Pcsk9 and angiopoietin-like 3 (Angptl3) using two doses of 5 mg RNP/kg.[16] In addition to a chemically synthesized nanoparticulate system, Banskota et al. reported engineered virus-like particles (eVLPs) containing base-editor RNPs. A single intravenous injection of the optimized fourth-generation eVLPs (7×10^{11} eVLPs) resulted in a 78% reduction in serum Pcsk9 levels.[17] We are developing Cas RNP-loaded LNPs composed of our original biodegradable ionizable lipid, CL4H6, and have demonstrated functional delivery of *Streptococcus pyrogenes* Cas9 (spCas9) and *Acidaminococcus* sp. Cas12a (AsCas12a) *in vitro*.[18] Recently, we demonstrated an approximately 80% reduction in serum TTR protein levels after two consecutive administrations of the Cas9 RNP-loaded LNPs at doses of 2 mg RNP/kg using the same ionizable lipid.[19] In this way, multiple reports on RNP-loaded nanoparticle formulations capable of RNP delivery and *in vivo* genome editing have been demonstrated. On the other hand, considering the enormous impact of genome editing, very few attempts have been made thus far, and much effort will be required to make it a reality for the treatment of disease.

RESULTS AND DISCUSSION

Design of novel ionizable lipids with different scaffold structures

Ionizable lipids, which are the main component in LNPs, have a tertiary amino moiety on their hydrophilic head group. The chemical structure of LNPs is known to have a significant impact on the acid dissociation constant (pKa) value. In the present study, a CL4 structure was adopted for the head group to establish a pKa range that would be suitable for the functional delivery of nucleic acids to liver parenchymal cells (hepatocytes), according to previous reports in the systematic library of ionizable lipids.[20,21] A hydrophobic scaffold creates a three-dimensional structure in ionizable lipids. A scaffold with a branched structure is known to exhibit superior functional delivery of mRNA compared with that accomplished using a linear structure.[20,22] Indeed, branched scaffold structures have been adopted for the clinically successful ionizable lipids ALC-0315 and SM-102, which are used in COVID-19 mRNA vaccines.[23] Our recent systematic structure-activity relationship (SAR) clearly revealed superior fusogenicity and functional delivery of mRNA for symmetrically branched scaffolds.[20] A branched scaffold structure is also known to maximize the ionization ability of ionizable lipids via a loss of lipid packing and improved physicochemical stability via an increase in the microviscosity of LNPs. While the branched scaffold is a useful substructure for the functional delivery of payloads, the ester bond in the α-branched structure is known to exhibit a limited degree of biodegradability.[24] Biodegradability of ionizable lipids is one of the promising strategies that is used to avoid ionizable lipid-derived toxicity.[21,25] Thus far, we have located neither reports regarding the engineering of ionizable lipids for the *in vivo* delivery of RNPs nor information on the appropriate branched scaffold structure. We hypothesized that both the branching position and total carbon number, which changes both the shape and bulkiness of a lipid, should affect the encapsulation state and the efficiency of functional delivery of RNPs, as well as the biodegradability. Based on this hypothesis, in this study we explored the optimal form of a branched ionizable lipid for the hepatic delivery of RNPs by developing a novel ionizable lipid library by focusing on the above parameters based on the previously synthesized benchmark ionizable lipid, CL4F6[20,21] (Figure 1A).

β-Branched, ε-branched, or more distant position-branched scaffolds (fatty acids) are adopted by considering the availability of raw materials and the ease of synthesis. The corresponding 1,4-unsaturated esters were obtained from symmetric ketones via the Horner-Wadsworth-Emmons (HWE) reaction, which then was followed by olefin reduction and alkaline hydrolysis to obtain β-branched fatty acids (Figure 1B). The yield above 100% after the HWE reactions is due to the fact that the reactant triethyl phosphonoacetate was not efficiently removed by the aliquoting operation and was contaminated. It was obvious that the separation of the target product and triethyl phosphonoacetate by column purification was relatively difficult, and also that the presence of triethyl phosphonoacetate had no crucial effect on the subsequent reaction so the separation from the final ionizable lipid was easy. Therefore, the reaction proceeded without excessive purification steps. Asymmetrically branched scaffolds were excluded because our previous studies have shown that asymmetrically branched scaffolds have limits to the positive effects described above compared with symmetrically branched scaffolds.[20] The effect of topology was examined by synthesizing six types of chain fatty acids and three types of cyclic fatty acids with total carbon numbers ranging from 9 to 19. Each synthesized β-branched fatty acid was condensed with common alkanolamine, CL4, to obtain the corresponding β-branched ionizable lipids (Figure 1A). The β-branched ionizable lipids are named CL4 (head) F (branched scaffold), which is followed by the "carbon number of main chain"_"branching position"-"carbon number of the side chain" (e.g., CL4F6_β-3). Fluc mRNA-loaded LNPs were first prepared to obtain the fundamental structure activity relationship (SAR) for β-branched ionizable lipids. Increases in the particle size and apparent pKa value and decreases in encapsulation efficiency were observed for lower carbon numbers (Table S3). The trend was more significant for circular

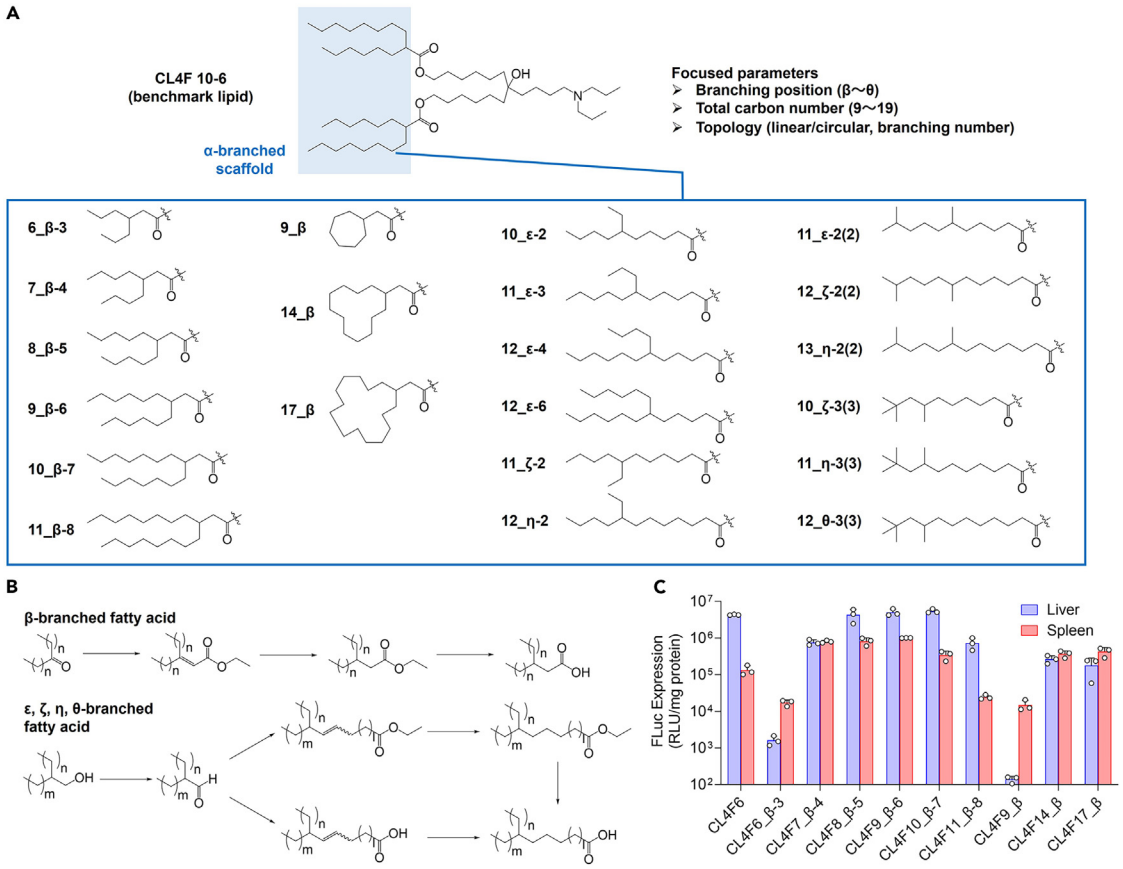

Figure 1. Synthesis of ionizable lipids with different branched scaffolds

(A) Variation of branched scaffolds synthesized in this study. Twenty-one types of branched ionizable lipids were designed focusing on the branching position, the total carbon number, and the topology. Previously reported α-branched ionizable lipid CL4F6 was used as a benchmark.

(B) General synthetic routes for the branched fatty acids.

(C) Fluc expression levels in the liver and spleen after intravenous injection of Fluc mRNA-loaded β-branched LNPs; $n = 3$.

scaffolds. Bell-shaped hepatic and splenic Fluc activity for the total carbon number of the ionized lipids with chain scaffolds was obtained after intravenous injection of the LNPs, which indicates that the optimal carbon number ranges from 13 to 17 (Figure 1C). The β-branched cyclic scaffolds showed significantly lower Fluc activity compared with that of the β-branched chain scaffolds with a consistent carbon number. Considering both the gene expression and the physical properties suggested that the chain scaffold contributed to the formation of stable particles with fewer carbons, and this setup stably delivered mRNA to both organs. In the case of chain scaffolds, each hydrocarbon chain efficiently interacts intermolecularly due to its high degree of freedom. Therefore, we concluded that the chain scaffold was a suitable structure for functional drug delivery and should be the focus of subsequent experiments.

Next, ε-branched fatty acids were synthesized (Figure 1B). First, α-branched aldehyde was obtained by the TEMPO oxidation of the corresponding branched alcohol. Then, the aldehydes were converted into the corresponding unsaturated esters or carboxylic acids. Finally, the desired ε-branched fatty acids were obtained by catalytic reduction followed by alkaline hydrolysis in the case of esters and were condensed with CL4 to obtain the corresponding ε-branched ionizable lipids (Figure 1A). With the exception of CL4F12_ε-6, the ε-branched ionizable lipids had asymmetric scaffolds due to the limitations of reagent availability. Similar to the β-branched LNPs, Fluc mRNA-loaded ε-branched LNPs were intravenously injected into mice to measure the functional delivery of mRNA in the liver and spleen. With the exception of CL4F10_ε-2, which had the lowest carbon number, three types of ε-branched LNPs showed hepatic Fluc expression levels comparable to that of CL4F6-LNPs (Figure S1). The stability of the CL4F10_ε-2-LNP was low due to its larger particle size and pKa by comparison with the others (Table S4).

Identification of ionizable lipids for hepatic ribonucleoprotein delivery

RNP-loaded LNPs targeting transthyretin (TTR) were prepared by selecting some of the synthesized ionized lipids (β-branched: 3 species, ε-branched: 3 species) (Table S5), and the serum TTR protein concentration was measured after intravenous administration to mice at 2 mg RNP/kg (Figure 2A, left). The previously used ionizable lipid CL4H6 and the benchmark for branched ionizable lipid, CL4F6, were used as controls. Newly synthesized ionizable lipids showed consistent or higher inhibition of serum TTR protein levels compared with the

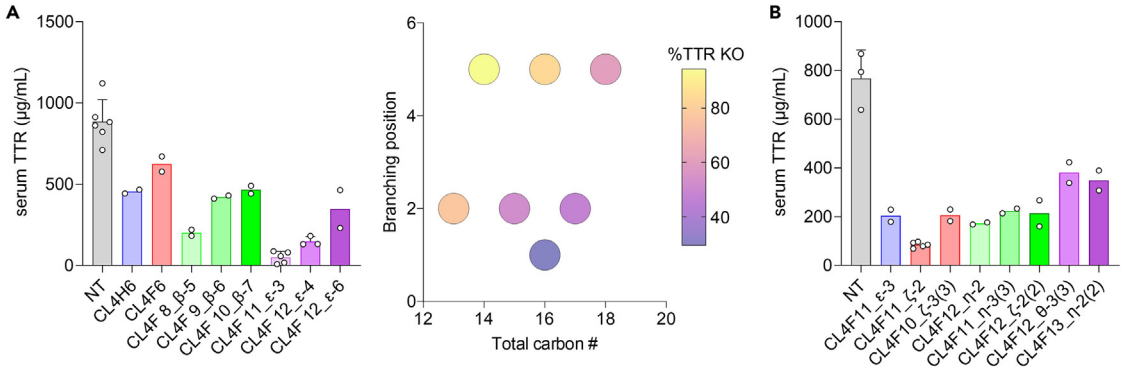

Figure 2. Screening of RNP-loaded LNPs with the synthesized branched ionizable lipid

(A) Initial screening using β- and ε-branched ionizable lipids. Serum TTR protein levels after TTR-targeting RNP-loaded LNPs were intravenously injected into mice at a dose of 2 mg RNP/kg. A bubble plot of the branching position, the total carbon number of scaffolds (total carbon #), and the %TTR protein knockout (KO) are expressed at right; n = 2–6.

(B) Second screening of additionally synthesized branched ionizable lipids. Serum TTR protein levels after TTR-targeting of RNP-loaded LNPs were intravenously injected into mice at a dose of 0.75 mg RNP/kg; n = 2–5.

control lipids. Interestingly, a clear trend was obtained wherein the farther the branching position and the lower the total carbon number of scaffolds, the higher the inhibitory rate of serum TTR protein (Figure 2A, right). CL4F11_ε-3-LNPs were the most active and achieved an inhibition rate of more than 90%, which indicates a substantial improvement in the functional delivery of RNPs in the liver compared with that of the control LNPs. Based on the SAR results, an additional seven types of ionizable lipids composed of scaffolds with total carbon numbers ranging from 13 to 15 and with branching positions that ranged from ε to θ were synthesized as a focused library to determine the optimal ionizable lipid structure (Figure 1A). Some of the additional ionizable lipids contained branched scaffolds with multiple side chains, and the structure was represented by indicating the branching position closest to the carbonyl carbon and the total number of the branches in parentheses (e.g., CL4F11_ε-2(2)). All of the additional branched LNPs exhibited a more than 50% inhibition of serum TTR protein after intravenous injection at 0.75 mg RNA/kg. The CL4F11_ζ-2-LNPs (ζ-LNPs) achieved the best TTR inhibition rate at more than 90% (Figures 2B; Table S6). Importantly, the inhibition rate seemed to be total carbon number-dependent, which supports the validity of the trend obtained from the previous experiment with β- and ε-branched lipids. The ζ-LNPs proved to be the optimal ionizable lipid for the functional delivery of RNPs in the liver. Although the formulation composition of the ζ-LNPs was examined, no obvious enhancement of the TTR inhibition rate was obtained (Figure S2). Therefore, the original composition was adopted in the following experiments.

In vivo performance of ζ-lipid nanoparticles

A dose-dependent study revealed that a 50% effective dose (ED_{50}) of the ζ-LNPs was 0.2 mg RNP/kg, which was approximately 10-fold lower than that for CL4H6-LNPs, and that a more than 98% inhibition of serum TTR protein was achieved at the highest dose (2 mg RNP/kg) (Figure 3A). The inhibitory rate was higher than that observed in a clinical study (87%),[5] strongly suggesting sufficient efficacy for obtaining a therapeutic effect. The reduced level of serum TTR protein was maintained for up to 12 weeks after a single injection of the ζ-LNPs (Figure 3B). Next-generation sequence (NGS) analysis revealed approximately 80% induction of insertion-deletion (indel) mutation at the target locus in whole liver genomic DNA (Figures 3C and S3). The insertion of thymidine, which is known as a characteristic of spCas9, was most frequently detected. A substantially low indel rate compared with that of the serum TTR protein inhibitory rate could be explained by the fact that the TTR gene encodes a protein specifically expressed in hepatocytes, while genomic DNA derives from the whole liver, which includes non-parenchymal cells and was used for NGS. Considering that only 60–70% of DNA copies in the whole liver are derived from hepatocytes,[26] we speculated that the ζ-LNPs induce genome editing in some non-parenchymal cells in addition to hepatocytes. To confirm that the ζ-LNPs could induce a knockout of different genes, the ζ-LNPs targeting two hepatocyte-specific genes, coagulation factor 9 (F9) and antithrombin (AT), were intravenously injected into mice at 2 mg RNP/kg (Figures 3D and 3E; Tables S7 and S8). Approximately 80 and 70% inhibition of plasma F9 activity and plasma AT protein level was observed in a target-specific manner, respectively.

To verify the potential of the CL4F11_ζ-2, a comparative study was performed using the clinically approved ionizable lipids DLin-MC3-DMA (MC3), SM-102, and ALC-0315 (Figures 3F; Table S9). An intravenous injection of RNP-loaded LNPs to mice at a dose of 0.75 mg RNP/kg revealed that CL4F11_ζ-2 shows an extremely strong inhibitory effect of serum TTR protein levels compared with all the approved ionizable lipids. MC3 had originally been identified as the optimal ionizable lipid for the delivery of siRNA to hepatocytes and has been used as a benchmark in many reports on mRNA delivery.[24,27,28] Although SM-102 and ALC-0315 had been developed as ionizable lipids for intramuscular mRNA vaccines, both are known to functionally deliver mRNA to the liver after intravenous injection.[29] Interestingly, the ζ-LNPs showed a relatively lower level of encapsulation efficiency, but changing the payload to Fluc mRNA significantly lowered gene expression levels in the liver compared with LNPs containing any other ionizable lipids (Table S10; Figure S4). This result, in which the order of functional delivery efficiency was completely different depending on the payload (RNP versus mRNA) — despite the same injection route and

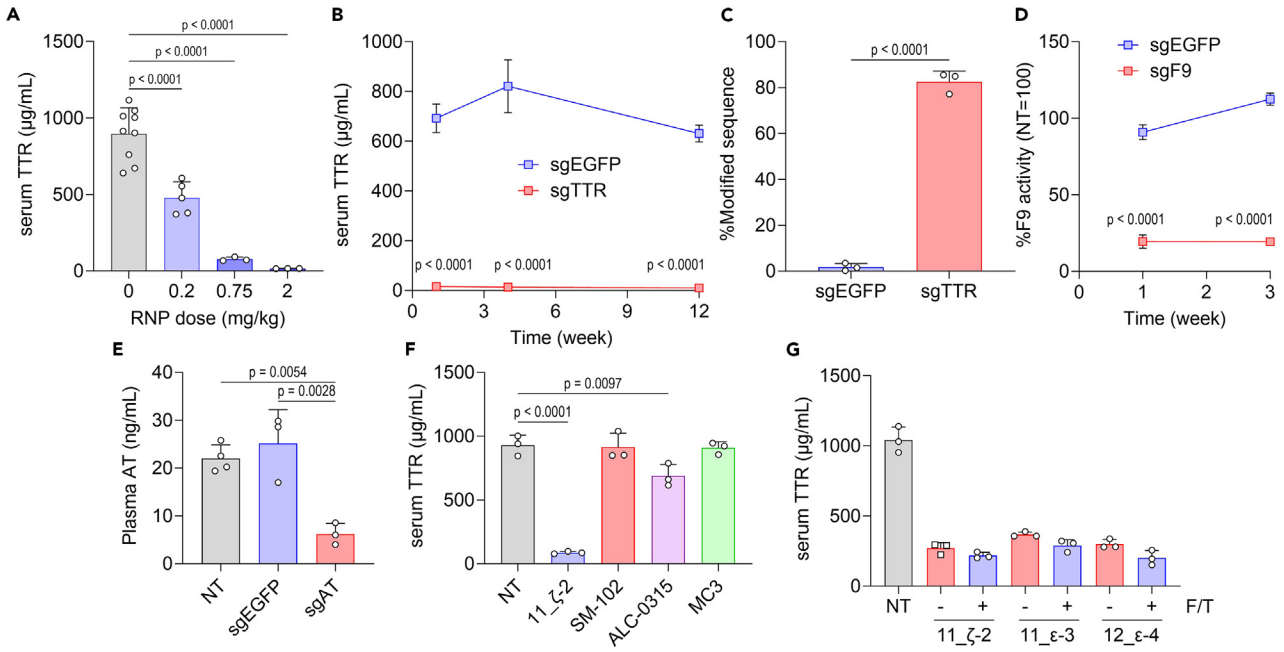

Figure 3. Performance of the RNP-loaded ζ-LNPs

(A) Dose-dependency of TTR protein inhibition 7 days after intravenous injection of ζ-LNPs; n = 3–9, Dunnett's test vs. 0 mg/kg.

(B) Durability of TTR protein inhibition after intravenous injection of ζ-LNPs at a dose of 2 mg RNP/kg; *n* = 3, unpaired Student's t test.

(C) Percentage of the modified sequence at the target genomic locus in whole liver tissue at 12 weeks after intravenous injection of ζ-LNPs at a dose of 2 mg RNP/kg; *n* = 3, unpaired Student's t test.

(D) Inhibitory effect of plasma F9 activity after intravenous injection of ζ-LNPs at a dose of 2 mg RNP/kg; *n* = 3, unpaired Student's t test.

(E) Inhibitory effect of plasma AT protein level after intravenous injection of ζ-LNPs at a dose of 1.5 mg RNP/kg; n = 3–4, Dunnett's test vs. NT.

(F) Comparison of TTR protein inhibition between LNPs containing CL4F11_ζ-2 and clinically approved ionizable lipids. TTR protein inhibition 7 days after an intravenous injection of RNP-loaded LNPs at a dose of 0.75 mg RNP/kg; *n* = 3, Dunnett's test vs. NT.

(G) Stability of RNP-loaded LNPs against a freeze-and-thaw (F/T) cycle. TTR protein inhibition 7 days after an intravenous injection of RNP-loaded LNPs before or after an F/T cycle at a dose of 0.75 mg RNP/kg; *n* = 3.

target organ — strongly reveals the differences in the interaction between LNP lipids and payloads and the internal structure of LNPs due to differences in the lipid structure and physical properties of the payload. The result also argues that the appropriate range and optimum values for the chemical structure and physical properties of ionizable lipids vary widely from payload to payload, which underscores the importance of optimizing the details according to the payload. As with the branched scaffold structure, the head structure is also assumed to play an important role in the functional delivery of RNPs in terms of interaction with RNPs. Further studies of the lipid structure, including the head structure, are warranted in the future.

Storage stability of the formulation is an important property to be considered for clinical application. Since Cas9 protein is a relatively large protein of about 160 kDa, it lacks a high level of thermostability. We have previously observed that, when optimized *in vitro*, RNP-loaded LNPs can be stored at 4°C for up to 2 weeks as a wet preparation, but after that time the titer decreases with no change in LNP properties, which suggests the instability of Cas9 protein.[18] Cryopreservation is an alternative and effective method for long-term storage of LNP formulations carrying unstable payloads and is in fact the method employed in COVID-19 mRNA vaccine formulations.[30,31] Non-reducible disaccharides such as sucrose and trehalose are generally used as cryoprotectants. In this study, the resistance to freeze-thaw of three LNPs, which includes ζ-LNPs, in the presence of sucrose was investigated. As a result, these LNPs showed neither obvious changes in physical properties nor a reduction in TTR knockout activity (Figures 3G; Table S11), which suggests the possibility of long-term storage in the frozen state.

CL4F11_ζ-2 is expected to be susceptible to degradation by esterases because the branching point of the scaffold is located away from the ester bond, and, therefore, the structure around the ester bond has a low level of bulk. Hepatic, splenic, and plasma concentrations of CL4F11_ζ-2 quantified by LC/MS after intravenous injection of the RNP-loaded LNPs rapidly decreased in a time-dependent manner, while we observed only a limited elimination of CL4F6, which has a bulky ester and was used as a negative control (Figures 4A–4C). Estimated decomposition products (monoacylated alkanolamines) derived from CL4F11_ζ-2 and CL4H6 (used as a positive control) were detected at early time points and decreased over time in both organs and plasma, which confirmed the cleavage of ester bonds (Figure S5). These results indicate that CL4F11_ζ-2 is biodegradable. These findings motivated us to examine the safety of ζ-LNPs. Both the serum biochemistry parameters and histopathological scores in the liver and spleen were determined 7 days after intravenous injection of the RNP-loaded ζ-LNPs at a dose of 2 mg RNP/kg (Figure 4D, 4E, and S6). Although there was a statistically significant increase in serum sodium ions and

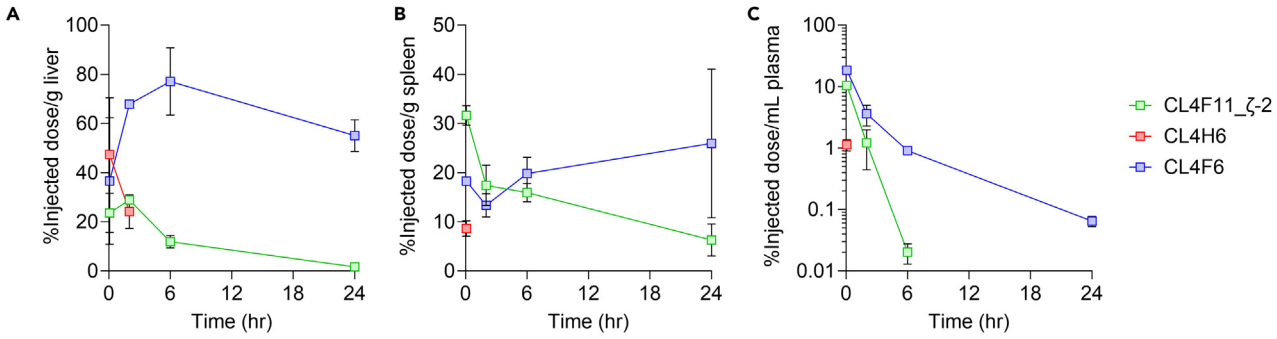

D

parameters	PBS	ζ-LNP	parameters	PBS	ζ-LNP
TP (g/dL)	4.7±0.2	4.8±0.1	ALT (IU/L)	31±3	29±5
ALB (g/dL)	3.3±0.2	3.2±0.0	LDH (IU/L)	248±76	297±70
BUN (mg/dL)	21.0±2.4	21.7±3.9	AMY (IU/L)	2098±226	2166±43
CRE (mg/dL)	0.16±0.01	0.17±0.01	γ-GT (IU/L)	<3	<3
Na (mEq/L)	152±1	153±1*	T-CHO (mg/dL)	70±5	76±5
K (mEq/L)	7.8±1.0	8.5±1.4	TG (mg/dL)	92±25	85±23
Cl (mEq/L)	110±1	109±1	HDL-C (mg/dL)	41±2	43±3
Ca (mg/dL)	9.6±0.2	9.9±0.5	T-BIL (mg/dL)	0.07±0.01	0.05±0.00
IP (mg/dL)	12.3±0.7	14.3±0.8*	GLU (mg/dL)	309±30	322±22
AST (IU/L)	53±4	58±4			

E

group	PBS				ζ-LNP			
mouse	1	2	3	4	1	2	3	4
Liver								
Abnormal findings	0	0	0	0	0	0	0	0
Spleen								
extramedullary hematopoiesis	0	0	1	0	1	1	1	1
enlargement of white splenic cord	0	0	0	1	0	1	0	1

Figure 4. Biocompatibility of the RNP-loaded ζ-LNPs

(A–C) Concentrations of ionizable lipids after an intravenous injection of RNP-loaded LNPs at a dose of 2 mg RNP/kg in the liver (A), spleen (B), and plasma (C) were quantified via LC/MS; n =3.

(D and E) Serum biochemistry parameters (D), and histopathological scores (E) 7 days after an intravenous injection of the RNP-loaded ζ-LNPs at a dose of 2 mg RNP/kg. Scores are indicated as follows: no abnormal findings (0), minor (1), moderate (2), intermediate (3), and high (4); $n = 4$, $*p < 0.05$ (unpaired Student's t test). TP: total protein; ALB: albumin; BUN: blood urea nitrogen; CRE: creatinine; IP: inorganic phosphates; AST: aspartate transaminase; ALT: alanine transaminase; LDH: lactose dehydrogenase; AMY: amylase; T-CHO: total cholesterol; TG: triglyceride; HDL-C: high-density lipoprotein cholesterol; T-BIL: total bilirubin; GLU: glucose.

in inorganic phosphate as well as an upward trend in histopathological scores in the spleen, there was no obvious sign of ζ-LNP-mediated toxicity.

Characterization of ζ-lipid nanoparticles

Cryo-TEM observation of the RNP-loaded ζ-LNPs revealed a "flower-like structure" with multiple blebs (or lobes) surrounding a core with a high electron density (Figures 5A and S7). Despite a lipid composition similar to typical RNA-loaded LNPs, it is assumed that the reason for the characteristic structure derives either from the chemical structure of CL4F11_ζ-2 itself or from the loading of the RNPs. No multiple blebs observed in RNP-loaded ζ-LNPs were found in siRNA-loaded ζ-LNPs (Figure 5B). In addition, electron-dense core structures surrounded by 0–2 small blebs were found in RNP-loaded CL4H6-LNPs (Figure 5C). These observations suggested that both the ionizable lipid structure and the loading of RNPs are involved in the "flower-like structure." Atomic force microscopy observation supported the unique structure of the RNP-loaded ζ-LNPs (Figure S8). A causal relationship between the flower-like structure and the efficiency of the functional delivery of RNPs would be controversial. While Cheng et al. reported the superior functional delivery of mRNA and the stability of mRNA-loaded LNPs containing blebs,[32] Goldman et al. developed HEPES-based ionizable lipids and found that the highly active mRNA-loaded LNPs show a relatively small electron-dense core structure with no blebs.[33] Thus, the relationship between the structure of LNPs, including blebs, and the degree of functional delivery is inconsistent and requires continued discussion. In any case, since the flower-like structure may alter the interaction with biological components, we first examined the ApoE-dependence on functional delivery. It is well known that intravenously injected liver-targeted LNPs adsorb ApoE proteins in the bloodstream and are then taken up by hepatocytes that express both highly sulfated heparansulfate proteoglycans (HSPGs) and LDLRs.[34,35] To clarify the relationship between ApoE-dependency, ionizable lipid structure, and payloads, the gene-knockout silencing activity of RNP- or siRNA-loaded CL4H6- or ζ-LNPs in wild-type and ApoE-deficient mice was measured (Figures 5D and 5E; Table S12). The inhibitory effect of plasma F7 activity decreased in ApoE-deficient mice for both forms of the siF7-loaded LNPs (Figure 5D), which indicates the ApoE-dependent hepatic delivery of siRNAs. On the other hand, there was no sign of a decrease in the inhibitory effect of serum TTR protein level for the RNP-loaded CL4H6-LNPs (Figure 5E). Rather, the TTR knockout activity of RNP-loaded ζ-LNPs significantly increased in ApoE-deficient mice. Our previous study showed that intravenously injected RNPs selectively accumulate in liver sinusoidal endothelial cells (LSECs),[19] and, therefore, RNPs exposed on the LNP interface are unlikely to guide LNPs to hepatocytes in an ApoE-independent manner. Therefore, a

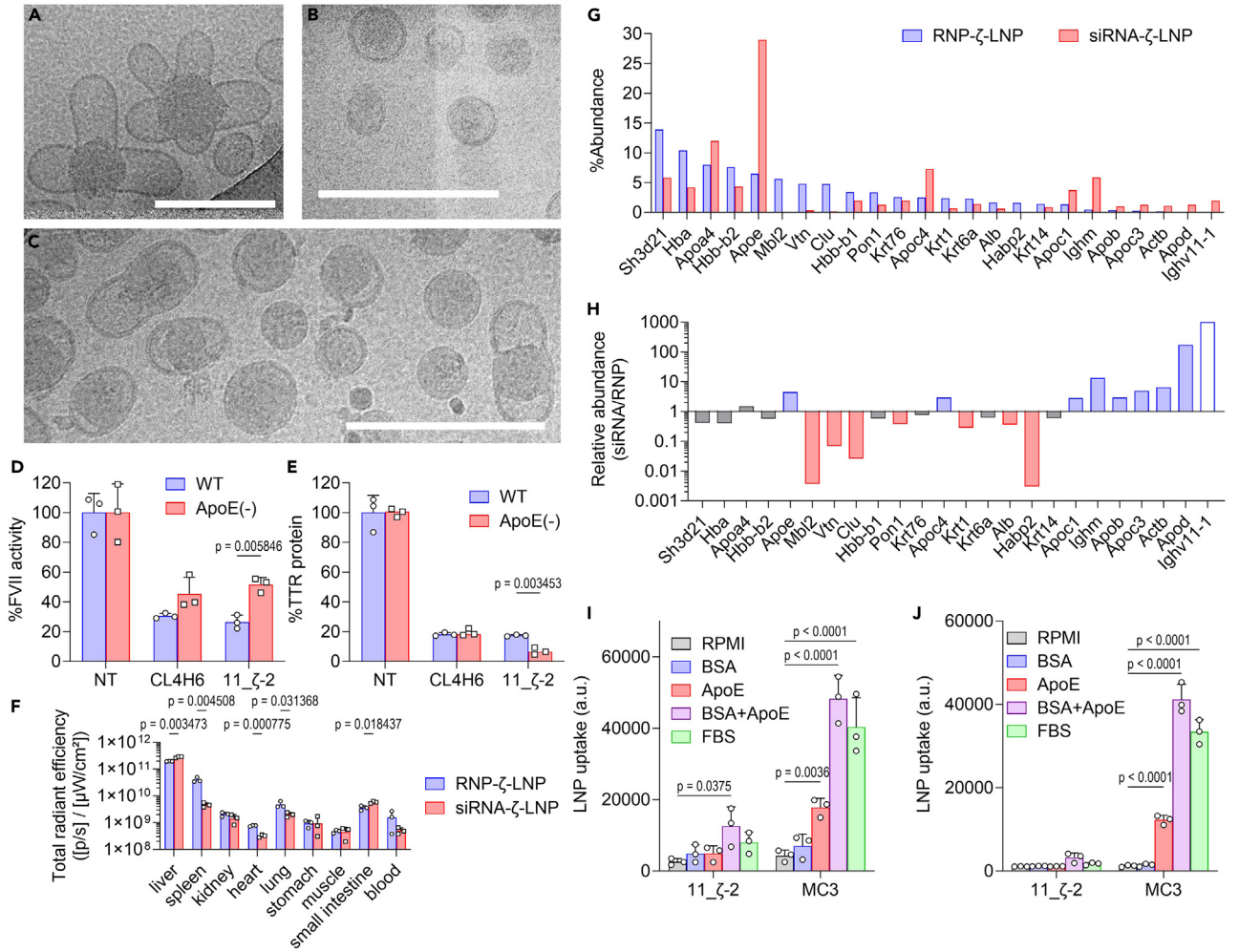

Figure 5. Characterization of the RNP-loaded ζ-LNPs

(A–C) Cryo-TEM observation of the RNP-loaded ζ-LNPs (A), siRNA-loaded ζ-LNPs (B), and RNP-loaded CL4H6-LNPs (C); Bars represent 200 nm.

(D) Relative plasma FVII activity in wild-type (WT) and ApoE-deficient mice 24 h after intravenous injection of siF7-loaded CL4H6- and ζ-LNPs at a dose of 0.2 mg siRNA/kg; *n* = 3, unpaired Student's t test.

(E) Relative serum TTR protein level in WT and ApoE-deficient mice 7 days after intravenous injection of sgTTR/Cas9 RNP-loaded CL4H6- and ζ-LNPs at doses of 2 and 0.75 mg RNP/kg, respectively; *n* = 3, unpaired Student's t test.

(F) Biodistribution of the RNP-loaded and siRNA-loaded ζ-LNPs measured by IVIS 1 h after intravenous injection at a dose of 0.75 mg RNP/kg and the DiR dose-matched siRNA dose, respectively; *n* = 3, unpaired Student's t test.

(G and H) Percentage of protein abundance from the protein corona of the RNP-loaded and siRNA-loaded ζ-LNPs. All proteins detected at a rate of 1% or more in any LNP are shown in the order of increasing number in the RNP-loaded ζ-LNPs (G). Enrichment rates of each protein to siRNA for RNPs are shown (H). Proteins detected up to 2.5-fold more or less in the siRNA-loaded ζ-LNPs are indicated in blue or red, respectively. Ighv11-1 was not detected in RNP-loaded ζ-LNPs, which is indicated by the open bar.

(I and J) *In vitro* cellular uptake of the RNP (I) or siRNA (J) -loaded ζ-LNPs and MC3-LNPs in either the absence or presence of the indicated proteins or FBS; *n* = 3, Dunnett's test vs. RPMI.

conformational change in LNPs is assumed to be associated with RNP loading that may have altered the protein corona. As approximately 80% of the injected RNP-loaded ζ-LNPs were eliminated from the bloodstream 1 h after injection (Figure S9), the biodistribution of the ζ-LNPs was evaluated at consistent time points. The RNP-loaded ζ-LNPs accumulated in the liver at a reduced amount compared with that of siRNA-loaded ζ-LNPs, and instead accumulated in the spleen, heart, and lungs (Figures 5F and S10), suggesting an alteration of the pharmacokinetics according to the type of payload. We then analyzed the protein corona of RNP-loaded ζ-LNPs and siRNA-loaded ζ-LNPs (Figure S11). Proteome analysis was conducted following the incubation of LNPs in freshly obtained mouse plasma followed by purifications (Figures 5G and 5H). The siRNA-loaded ζ-LNPs were dominated by the top three apolipoproteins (ApoE, ApoA4, and ApoC4), which is similar to other hepatotropic LNPs.[36,37] The Apolipoprotein-rich composition appeared consistent with the results of

ApoE-dependent functional siRNA delivery. As expected, the RNP-loaded LNPs showed a completely different protein composition compared with that of the siRNA-loaded LNPs. With the exception of Clu (ApoJ), the amount of all detected apolipoproteins had clearly decreased, while Mbl2, Vtn, Clu, Alb, and Habp showed a high rate of increase. Mbl2 and Vtn are known to be ligands against C1q receptor and are believed to contribute to its high accumulation in the spleen.[38,39] Vtn has an Arg-Gly-Asp (RGD) motif and is reported to function as a ligand against the $\alpha_v\beta_3$ integrin expressed in lung endothelial cells and to contribute to an increased accumulation in the lungs.[36] Clu is a ubiquitously expressed 70 kDa multifunctional glycoprotein that is known to inhibit amyloid formation and to prevent the stress-induced aggregation of plasma proteins as an extracellular molecular chaperone protein. Clu is a ligand for ApoER2 and VLDLR,[40,41] but neither receptor is expressed in the liver.[42] On the other hand, hepatocyte-selective uptake of client proteins via fucoidan-inhibitory scavenger-like receptors has been reported.[43] Alb is a ligand for glycoprotein scavenger receptors gp18 and gp30, and is reported to be an uptake mechanism for LNPs composed of both cKK-E12 and A6 ionizable lipids into hepatocytes.[44] Habp2 may contribute to the affinity of the LNPs for LSECs, which are responsible for the blood clearance of hyaluronan through the high expression of hyaluronan receptors (CD44, HARE, STAB2, and LYVE-1) by virtue of their hyaluronan-binding activity.[45–47] ApoE and Alb are reported to be involved in LNP uptake into hepatocytes, and we examined their contribution to the cellular uptake of ζ-LNPs. MC3-LNPs are known to exhibit ApoE-dependent uptake to hepatocytes and were used for a comparison.[48] The MC3-LNPs showed a marked increase in uptake with the addition of ApoE, but not with the addition of Alb (Figures 5I and 5J; Table S13). Surprisingly, the co-addition of ApoE and Alb showed uptake that approximated that of the positive control, FBS. Confocal laser scanning microscopy observation confirmed the internalization of the RNP-loaded ζ-LNPs (Figure S12). Negligible cytotoxicity was also confirmed in the tested range of lipid concentration (Figure S13). Since Alb is known to interact with a variety of proteins, including ApoE,[49] it may have had a synergistic effect. For the ζ-LNPs, the increase in uptake by ApoE was limited, which is consistent with the results of *in vivo* TTR inhibition and proteomic analysis. Nevertheless, the co-addition of ApoE and Alb caused a definite increase in uptake, but the level was markedly lower compared with that of the MC3-LNPs. In contrast to *in vivo* observation, siRNA-loaded ζ-LNPs showed no increase in uptake following ApoE addition (Figure 5J). This suggests that the presence of ApoE is a necessary, albeit insufficient, condition. The simple *in vitro* conditions may limit our understanding of the *in vivo* uptake mechanism, since *in vivo* distribution is determined by the ensemble of diverse proteins, as when the co-addition of ApoE and Alb caused an increase in the uptake.[50] On the other hand, the clear evidence of changes in the LNP structure due to the scaffold structure of ionizable lipids and the loading of RNPs, protein corona, and uptake mechanisms will contribute to the understanding and control of future nanoparticle-biomolecule interactions.

Limitations of study

The SAR study revealed both total carbon numbers and branching positions of the scaffold structure of ionizable lipids are critical factors for the hepatic delivery of RNPs. However, this finding is limited in CL4F-based backbone structure and in hepatocytes. Further examinations should be conducted to generalize SAR and to widen targetable organs/cells. In addition, the reason why the quality of protein corona and apoE-dependency are significantly affected by a type of payload (siRNA vs. RNP) is not clarified yet. Deeper examinations of fluidity, 3-dimensional structure, orientation, and arrangement of both lipids and RNPs are required for an intrinsic understanding of the reason and for the rational design of RNP-loaded LNPs.

RESOURCE AVAILABILITY

Lead contact

Additional information and requests for resources and reagents used in this study should be directed to and will be fulfilled by the lead contact, Yusuke Sato (y_sato@pharm.hokudai.ac.jp).

Materials availability

All unique/stable reagents generated in this study are available from the lead contact with a completed Materials Transfer Agreement.

Data and code availability

- Data: All data reported in this article will be shared by the lead contact upon request. The mass spectrometry experiments presented in this study have been deposited to the ProteomeXchange Consortium (http://www.proteomexchange.org/) (accession number: PXD055572).
- Code: This article does not report the original code.
- Any additional information required to reanalyze the data reported in this article is available from the lead contact upon request.

ACKNOWLEDGMENTS

This work was supported, in part, by Special Education and Research Expenses from the Ministry of Education, Culture, Sports, Science and Technology, Hokkaido University Support Program for Frontier Research, JSPS KAKENHI Grant Number JP23H03732, AMED under Grant Number JP23bm1223004h0001; and, from the TERUMO LIFE SCIENCE FOUNDATION. The authors wish to thank Prof. Manabu Tokeshi and Assoc. prof. Masatosi Maeki from the graduate school of engineering at Hokkaido University for kindly providing an iLiNP microfluidic device. The authors also wish to thank Dr. James McDonald for his helpful advice in preparing the English article.

AUTHOR CONTRIBUTIONS

Conceptualization and methodology: Y.Sa.; validation: Y.Sa.; formal analysis: H.O. and Y.Sa.; investigation: H.O., R.S., Y.Su., M.S., and Y.Sa.; resources: H.O. and Y.Sa.; writing – original draft: Y.Sa.; writing –review and editing: H.O., R.S., and Y.Sa.; visualization: Y.Sa.; supervision: Y.Sa. and H.H.; project administration: Y.Sa.; funding acquisition: Y.Sa. and H.H.

DECLARATION OF INTERESTS

H.O., Y.Sa., and H.H. are the authors of patent appl. No. PCT/JP2023/003844, which is relative to this study.

STAR★METHODS

Detailed methods are provided in the online version of this paper and include the following:

SUPPLEMENTAL INFORMATION

Supplemental information can be found online at https://doi.org/10.1016/j.isci.2024.110928.

Received: April 17, 2024
Revised: July 25, 2024
Accepted: September 9, 2024
Published: September 11, 2024

REFERENCES

1. Jinek, M., Chylinski, K., Fonfara, I., Hauer, M., Doudna, J.A., and Charpentier, E. (2012). A programmable dual-RNA-guided DNA endonuclease in adaptive bacterial immunity. Science *337*, 816–821. https://doi.org/10.1126/science.1225829.
2. Lim, J.M., and Kim, H.H. (2022). Basic Principles and Clinical Applications of CRISPR-Based Genome Editing. Yonsei Med. J. *63*, 105–113. https://doi.org/10.3349/ymj.2022.63.2.105.
3. Tang, X., Zhang, Y., and Han, X. (2023). Ionizable Lipid Nanoparticles for mRNA Delivery. Advanced NanoBiomed Research *3*, 2300006. https://doi.org/10.1002/anbr.202300006.
4. Zhang, Y., Sun, C., Wang, C., Jankovic, K.E., and Dong, Y. (2021). Lipids and Lipid Derivatives for RNA Delivery. Chem. Rev. *121*, 12181–12277. https://doi.org/10.1021/acs.chemrev.1c00244.
5. Gillmore, J.D., Gane, E., Taubel, J., Kao, J., Fontana, M., Maitland, M.L., Seitzer, J., O'Connell, D., Walsh, K.R., Wood, K., et al. (2021). CRISPR-Cas9 In Vivo Gene Editing for Transthyretin Amyloidosis. N. Engl. J. Med. *385*, 493–502. https://doi.org/10.1056/NEJMoa2107454.
6. Longhurst, H.J., Lindsay, K., Petersen, R.S., Fijen, L.M., Gurugama, P., Maag, D., Butler, J.S., Shah, M.Y., Golden, A., Xu, Y., et al. (2024). CRISPR-Cas9 In Vivo Gene Editing of KLKB1 for Hereditary Angioedema. N. Engl. J. Med. *390*, 432–441. https://doi.org/10.1056/NEJMoa2309149.
7. Lin, Y., Wagner, E., and Lächelt, U. (2022). Non-viral delivery of the CRISPR/Cas system: DNA. Biomater. Sci. *10*, 1166–1192. https://doi.org/10.1039/d1bm01658j.
8. Liang, X., Potter, J., Kumar, S., Zou, Y., Quintanilla, R., Sridharan, M., Carte, J., Chen, W., Roark, N., Ranganathan, S., et al. (2015). Rapid and highly efficient mammalian cell engineering via Cas9 protein transfection. J. Biotechnol. *208*, 44–53. https://doi.org/10.1016/j.jbiotec.2015.04.024.
9. Leibowitz, M.L., Papathanasiou, S., Doerfler, P.A., Blaine, L.J., Sun, L., Yao, Y., Zhang, C.Z., Weiss, M.J., and Pellman, D. (2021). Chromothripsis as an on-target consequence of CRISPR-Cas9 genome editing. Nat. Genet. *53*, 895–905. https://doi.org/10.1038/s41588-021-00838-7.
10. Enache, O.M., Rendo, V., Abdusamad, M., Lam, D., Davison, D., Pal, S., Currimjee, N., Hess, J., Pantel, S., Nag, A., et al. (2020). Cas9 activates the p53 pathway and selects for p53-inactivating mutations. Nat. Genet. *52*, 662–668. https://doi.org/10.1038/s41588-020-0623-4.
11. Kenjo, E., Hozumi, H., Makita, Y., Iwabuchi, K.A., Fujimoto, N., Matsumoto, S., Kimura, M., Amano, Y., Ifuku, M., Naoe, Y., et al. (2021). Low immunogenicity of LNP allows repeated administrations of CRISPR-Cas9 mRNA into skeletal muscle in mice. Nat. Commun. *12*, 7101. https://doi.org/10.1038/s41467-021-26714-w.
12. Kagita, A., Lung, M.S.Y., Xu, H., Kita, Y., Sasakawa, N., Iguchi, T., Ono, M., Wang, X.H., Gee, P., and Hotta, A. (2021). Efficient ssODN-Mediated Targeting by Avoiding Cellular Inhibitory RNAs through Precomplexed CRISPR-Cas9/sgRNA Ribonucleoprotein. Stem Cell Rep. *16*, 985–996. https://doi.org/10.1016/j.stemcr.2021.02.013.
13. Behr, M., Zhou, J., Xu, B., and Zhang, H. (2021). delivery of CRISPR-Cas9 therapeutics: Progress and challenges. Acta Pharm. Sin. B *11*, 2150–2171. https://doi.org/10.1016/j.apsb.2021.05.020.
14. Wei, T., Cheng, Q., Min, Y.L., Olson, E.N., and Siegwart, D.J. (2020). Systemic nanoparticle delivery of CRISPR-Cas9 ribonucleoproteins for effective tissue specific genome editing. Nat. Commun. *11*, 3232. https://doi.org/10.1038/s41467-020-17029-3.
15. Lee, K., Conboy, M., Park, H.M., Jiang, F., Kim, H.J., Dewitt, M.A., Mackley, V.A., Chang, K., Rao, A., Skinner, C., et al. (2017). Nanoparticle delivery of Cas9 ribonucleoprotein and donor DNA. Nat. Biomed. Eng. *1*, 889–901. https://doi.org/10.1038/s41551-017-0137-2.
16. Gong, J., Wang, H.X., Lao, Y.H., Hu, H., Vatan, N., Guo, J., Ho, T.C., Huang, D., Li, M., Shao, D., and Leong, K.W. (2020). A Versatile Nonviral Delivery System for Multiplex Gene-Editing in the Liver. Adv. Mater. *32*, e2003537. https://doi.org/10.1002/adma.202003537.
17. Banskota, S., Raguram, A., Suh, S., Du, S.W., Davis, J.R., Choi, E.H., Wang, X., Nielsen, S.C., Newby, G.A., Randolph, P.B., et al. (2022). Engineered virus-like particles for efficient in vivo delivery of therapeutic proteins. Cell *185*, 250–265.e16. https://doi.org/10.1016/j.cell.2021.12.021.
18. Suzuki, Y., Onuma, H., Sato, R., Sato, Y., Hashiba, A., Maeki, M., Tokeshi, M., Kayesh, M.E.H., Kohara, M., Tsukiyama-Kohara, K., and Harashima, H. (2021). Lipid nanoparticles loaded with ribonucleoprotein-oligonucleotide complexes synthesized using a microfluidic device exhibit robust genome editing and hepatitis B virus inhibition. J. Contr. Release *330*, 61–71. https://doi.org/10.1016/j.jconrel.2020.12.013.
19. Onuma, H., Sato, Y., and Harashima, H. (2023). Lipid nanoparticle-based ribonucleoprotein delivery for in vivo genome editing. J. Contr. Release *355*, 406–416. https://doi.org/10.1016/j.jconrel.2023.02.008.
20. Hashiba, K., Sato, Y., Taguchi, M., Sakamoto, S., Otsu, A., Maeda, Y., Shishido, T., Murakawa, M., Okazaki, A., and Harashima, H. (2023). Branching Ionizable Lipids Can Enhance the Stability, Fusogenicity, and Functional Delivery of mRNA. Small Science *3*, 2200071. https://doi.org/10.1002/smsc.202200071.
21. Sato, Y., Hashiba, K., Sasaki, K., Maeki, M., Tokeshi, M., and Harashima, H. (2019). Understanding structure-activity relationships of pH-sensitive cationic lipids facilitates the rational identification of promising lipid nanoparticles for delivering siRNAs in vivo. J. Contr. Release *295*, 140–152. https://doi.org/10.1016/j.jconrel.2019.01.001.
22. Hajj, K.A., Ball, R.L., Deluty, S.B., Singh, S.R., Strelkova, D., Knapp, C.M., and Whitehead, K.A. (2019). Branched-Tail Lipid Nanoparticles Potently Deliver mRNA In Vivo due to Enhanced Ionization at Endosomal pH. Small *15*, e1805097. https://doi.org/10.1002/smll.201805097.
23. Buschmann, M.D., Carrasco, M.J., Alishetty, S., Paige, M., Alameh, M.G., and Weissman, D. (2021). Nanomaterial Delivery Systems for mRNA Vaccines. Vaccines *9*, 65.
24. Sabnis, S., Kumarasinghe, E.S., Salerno, T., Mihai, C., Ketova, T., Senn, J.J., Lynn, A., Bulychev, A., McFadyen, I., Chan, J., et al. (2018). A Novel Amino Lipid Series for mRNA Delivery: Improved Endosomal Escape and Sustained Pharmacology and Safety in Non-human Primates. Mol. Ther. *26*, 1509–1519. https://doi.org/10.1016/j.ymthe.2018.03.010.
25. Maier, M.A., Jayaraman, M., Matsuda, S., Liu, J., Barros, S., Querbes, W., Tam, Y.K., Ansell, S.M., Kumar, V., Qin, J., et al. (2013). Biodegradable lipids enabling rapidly eliminated lipid nanoparticles for systemic delivery of RNAi therapeutics. Mol. Ther. *21*, 1570–1578. https://doi.org/10.1038/mt.2013.124.
26. Yin, H., Song, C.-Q., Dorkin, J.R., Zhu, L.J., Li, Y., Wu, Q., Park, A., Yang, J., Suresh, S., Bizhanova, A., et al. (2016). Therapeutic genome editing by combined viral and non-viral delivery of CRISPR system components in vivo. Nat. Biotechnol. *34*, 328–333. https://doi.org/10.1038/nbt.3471.
27. Jayaraman, M., Ansell, S.M., Mui, B.L., Tam, Y.K., Chen, J., Du, X., Butler, D., Eltepu, L., Matsuda, S., Narayanannair, J.K., et al. (2012). Maximizing the potency of siRNA lipid nanoparticles for hepatic gene silencing in vivo. Angew Chem. Int. Ed. Engl. *51*, 8529–8533. https://doi.org/10.1002/anie.201203263.
28. Yanez Arteta, M., Kjellman, T., Bartesaghi, S., Wallin, S., Wu, X., Kvist, A.J., Dabkowska, A., Székely, N., Radulescu, A., Bergenholtz, J., and Lindfors, L. (2018). Successful reprogramming of cellular protein production through mRNA delivered by functionalized lipid nanoparticles. Proc. Natl. Acad. Sci. USA *115*, E3351–E3360. https://doi.org/10.1073/pnas.1720542115.
29. Maeki, M., Okada, Y., Uno, S., Sugiura, K., Suzuki, Y., Okuda, K., Sato, Y., Ando, M.,

Yamazaki, H., Takeuchi, M., et al. (2023). Mass production system for RNA-loaded lipid nanoparticles using piling up microfluidic devices. Appl. Mater. Today *31*, 101754. https://doi.org/10.1016/j.apmt.2023.101754.
30. Zhao, P., Hou, X., Yan, J., Du, S., Xue, Y., Li, W., Xiang, G., and Dong, Y. (2020). Long-term storage of lipid-like nanoparticles for mRNA delivery. Bioact. Mater. *5*, 358–363. https://doi.org/10.1016/j.bioactmat.2020.03.001.
31. Kim, B., Hosn, R.R., Remba, T., Yun, D., Li, N., Abraham, W., Melo, M.B., Cortes, M., Li, B., Zhang, Y., et al. (2023). Optimization of storage conditions for lipid nanoparticle-formulated self-replicating RNA vaccines. J. Contr. Release *353*, 241–253. https://doi.org/10.1016/j.jconrel.2022.11.022.
32. Cheng, M.H.Y., Leung, J., Zhang, Y., Strong, C., Basha, G., Momeni, A., Chen, Y., Jan, E., Abdolahzadeh, A., Wang, X., et al. (2023). Induction of Bleb Structures in Lipid Nanoparticle Formulations of mRNA Leads to Improved Transfection Potency. Adv. Mater. *35*, e2303370. https://doi.org/10.1002/adma.202303370.
33. Goldman, R.L., Vittala Murthy, N.T., Northen, T.P., Balakrishnan, A., Chivukula, S., Danz, H., Tibbitts, T., Dias, A., Vargas, J., Cooper, D., et al. (2023). Understanding structure activity relationships of Good HEPES lipids for lipid nanoparticle mRNA vaccine applications. Biomaterials *301*, 122243. https://doi.org/10.1016/j.biomaterials.2023.122243.
34. Akinc, A., Querbes, W., De, S., Qin, J., Frank-Kamenetsky, M., Jayaprakash, K.N., Jayaraman, M., Rajeev, K.G., Cantley, W.L., Dorkin, J.R., et al. (2010). Targeted delivery of RNAi therapeutics with endogenous and exogenous ligand-based mechanisms. Mol. Ther. *18*, 1357–1364. https://doi.org/10.1038/mt.2010.85.
35. Sato, Y., Kinami, Y., Hashiba, K., and Harashima, H. (2020). Different kinetics for the hepatic uptake of lipid nanoparticles between the apolipoprotein E/low density lipoprotein receptor and the N-acetyl-d-galactosamine/asialoglycoprotein receptor pathway. J. Contr. Release *322*, 217–226. https://doi.org/10.1016/j.jconrel.2020.03.006.
36. Dilliard, S.A., Cheng, Q., and Siegwart, D.J. (2021). On the mechanism of tissue-specific mRNA delivery by selective organ targeting nanoparticles. Proc. Natl. Acad. Sci. USA *118*, e2109256118. https://doi.org/10.1073/pnas.2109256118.
37. Qiu, M., Tang, Y., Chen, J., Muriph, R., Ye, Z., Huang, C., Evans, J., Henske, E.P., and Xu, Q. (2022). Lung-selective mRNA delivery of synthetic lipid nanoparticles for the treatment of pulmonary lymphangioleiomyomatosis. Proc. Natl. Acad. Sci. USA *119*, e2116271119. https://doi.org/10.1073/pnas.2116271119.
38. Lim, B.-L., Reid, K.B., Ghebrehiwet, B., Peerschke, E.I., Leigh, L.A., and Preissner, K.T. (1996). The Binding Protein for Globular Heads of Complement C1q, gC1qR: FUNCTIONAL EXPRESSION AND CHARACTERIZATION AS A NOVEL VITRONECTIN BINDING FACTOR. J. Biol. Chem. *271*, 26739–26744. https://doi.org/10.1074/jbc.271.43.26739.
39. Ghebrehiwet, B., and Peerschke, E.I.B. (2004). cC1q-R (calreticulin) and gC1q-R/p33: ubiquitously expressed multi-ligand binding cellular proteins involved in inflammation and infection. Mol. Immunol. *41*, 173–183. https://doi.org/10.1016/j.molimm.2004.03.014.
40. Leeb, C., Eresheim, C., and Nimpf, J. (2014). Clusterin is a ligand for apolipoprotein E receptor 2 (ApoER2) and very low density lipoprotein receptor (VLDLR) and signals via the Reelin-signaling pathway. J. Biol. Chem. *289*, 4161–4172. https://doi.org/10.1074/jbc.M113.529271.
41. Dlugosz, P., and Nimpf, J. (2018). The Reelin Receptors Apolipoprotein E receptor 2 (ApoER2) and VLDL Receptor. Int. J. Mol. Sci. *19*, 3090. https://doi.org/10.3390/ijms19103090.
42. Oka, K., Ishimura-Oka, K., Chu, M.J., Sullivan, M., Krushkal, J., Li, W.H., and Chan, L. (1994). Mouse very-low-density-lipoprotein receptor (VLDLR) cDNA cloning, tissue-specific expression and evolutionary relationship with the low-density-lipoprotein receptor. Eur. J. Biochem. *224*, 975–982. https://doi.org/10.1111/j.1432-1033.1994.00975.x.
43. Wyatt, A.R., Yerbury, J.J., Berghofer, P., Greguric, I., Katsifis, A., Dobson, C.M., and Wilson, M.R. (2011). Clusterin facilitates in vivo clearance of extracellular misfolded proteins. Cell. Mol. Life Sci. *68*, 3919–3931. https://doi.org/10.1007/s00018-011-0684-8.
44. Miao, L., Lin, J., Huang, Y., Li, L., Delcassian, D., Ge, Y., Shi, Y., and Anderson, D.G. (2020). Synergistic lipid compositions for albumin receptor mediated delivery of mRNA to the liver. Nat. Commun. *11*, 2424. https://doi.org/10.1038/s41467-020-16248-y.
45. Falkowski, M., Schledzewski, K., Hansen, B., and Goerdt, S. (2003). Expression of stabilin-2, a novel fasciclin-like hyaluronan receptor protein, in murine sinusoidal endothelia, avascular tissues, and at solid/liquid interfaces. Histochem. Cell Biol. *120*, 361–369. https://doi.org/10.1007/s00418-003-0585-5.
46. Carreira, C.M., Nasser, S.M., di Tomaso, E., Padera, T.P., Boucher, Y., Tomarev, S.I., and Jain, R.K. (2001). LYVE-1 Is Not Restricted to the Lymph Vessels: Expression in Normal Liver Blood Sinusoids and Down-Regulation in Human Liver Cancer and Cirrhosis1. Cancer Res. *61*, 8079–8084.
47. Zhou, B., Weigel, J.A., Fauss, L., and Weigel, P.H. (2000). Identification of the hyaluronan receptor for endocytosis (HARE). J. Biol. Chem. *275*, 37733–37741. https://doi.org/10.1074/jbc.M003030200.
48. Sebastiani, F., Yanez Arteta, M., Lerche, M., Porcar, L., Lang, C., Bragg, R.A., Elmore, C.S., Krishnamurthy, V.R., Russell, R.A., Darwish, T., et al. (2021). Apolipoprotein E Binding Drives Structural and Compositional Rearrangement of mRNA-Containing Lipid Nanoparticles. ACS Nano *15*, 6709–6722. https://doi.org/10.1021/acsnano.0c10064.
49. Gundry, R.L., Fu, Q., Jelinek, C.A., Van Eyk, J.E., and Cotter, R.J. (2007). Investigation of an albumin-enriched fraction of human serum and its albuminome. Proteomics. Clin. Appl. *1*, 73–88. https://doi.org/10.1002/prca.200600276.
50. Dilliard, S.A., Sun, Y., Brown, M.O., Sung, Y.-C., Chatterjee, S., Farbiak, L., Vaidya, A., Lian, X., Wang, X., Lemoff, A., and Siegwart, D.J. (2023). The interplay of quaternary ammonium lipid structure and protein corona on lung-specific mRNA delivery by selective organ targeting (SORT) nanoparticles. J. Contr. Release *361*, 361–372. https://doi.org/10.1016/j.jconrel.2023.07.058.
51. Kimura, N., Maeki, M., Sato, Y., Note, Y., Ishida, A., Tani, H., Harashima, H., and Tokeshi, M. (2018). Development of the iLiNP Device: Fine Tuning the Lipid Nanoparticle Size within 10 nm for Drug Delivery. ACS Omega *3*, 5044–5051. https://doi.org/10.1021/acsomega.8b00341.
52. Hashiba, A., Toyooka, M., Sato, Y., Maeki, M., Tokeshi, M., and Harashima, H. (2020). The use of design of experiments with multiple responses to determine optimal formulations for in vivo hepatic mRNA delivery. J. Contr. Release *327*, 467–476. https://doi.org/10.1016/j.jconrel.2020.08.031.
53. Sato, Y., Hatakeyama, H., Sakurai, Y., Hyodo, M., Akita, H., and Harashima, H. (2012). A pH-sensitive cationic lipid facilitates the delivery of liposomal siRNA and gene silencing activity in vitro and in vivo. J. Contr. Release *163*, 267–276. https://doi.org/10.1016/j.jconrel.2012.09.009.
54. Sato, Y., Matsui, H., Yamamoto, N., Sato, R., Munakata, T., Kohara, M., and Harashima, H. (2017). Highly specific delivery of siRNA to hepatocytes circumvents endothelial cell-mediated lipid nanoparticle-associated toxicity leading to the safe and efficacious decrease in the hepatitis B virus. J. Contr. Release *266*, 216–225. https://doi.org/10.1016/j.jconrel.2017.09.044.

STAR★METHODS

KEY RESOURCES TABLE

REAGENT or RESOURCE	SOURCE	IDENTIFIER
Chemicals, peptides, and recombinant proteins		
TrueCut Cas9 Protein v2	Thermo Fisher Scientific	Cat#A36499
Cholesterol Sigma Grade, ≥99%	Sigma-Aldrich	Cat#C8667-5G
1,2-distearoyl-sn-glycero-3-phosphatidylcholine	NOF AMERICA CORPORATION	Cat#MC-8080
1,2-Dimyristoyl-rac-glycero-3-methylpolyoxyethylene	NOF AMERICA CORPORATION	Cat#GM-020
SM-102	Cayman Chemical	Cat#33474
ALC-0315	Ambeed	Cat#A1375212-100 mg
D-Lin-MC3-DMA	Selleck Biotech	Cat#S6683
DiR′; DiIC$_{18}$(7) 1,1′-Dioctadecyl-3,3,3′,3′-Tetramethylindotricarbocyanine Iodide	Thermo Fisher Scientific	Cat#D12731
DiD′ solid; DiIC$_{18}$(5) solid (1,1′-Dioctadecyl-3,3,3′,3′-Tetramethylindodicarbocyanine, 4-Chlorobenzenesulfonate Salt)	Thermo Fisher Scientific	Cat#D7757
6-(p-toluidino)-2-naphthalenesulfonic acid sodium salt	Sigma-Aldrich	Cat#T9792-250MG
Apolipoprotein E3(ApoE3), Human, recombinant	Wako	Cat#010-20261
Albumin, from Bovine Serum, Fraction V pH7.0	Wako	Cat# 015-27053
Hoechst 33342 solution	Wako	Cat#H342
Quant-iT RiboGreen RNA Reagent	Thermo Fisher Scientific	Cat#R11491
Critical commercial assays		
Prealbumin ELISA Kit (Mouse)	Aviva systems Biology	Cat#OKIA00111
Mouse Antithrombin III ELISA Kit (SERPINC1)	Abcam	Cat#ab108800
Revohem FIX Chromogenic Measurement Kit	sysmex	BD-496-632
BIOPHEN FVII	HYPHEN BioMed	Cat#221304
ReadyPrep 2-D Cleanup Kit	BIO-RAD	Cat# 1632130
CBQCA Protein Quantitation Kit	Thermo Fisher Scientific	Cat#C6667
Cell Counting Kit-8	DOJINDO	Cat#341-07761
Nano-Glo Luciferase assay system	Promega	Cat#N1110
Deposited data		
The mass spectrometry data	ProteomeXchange Consortium	PXD055572
Experimental models: Cell lines		
Hepa1c1c7	ATCC	CRL-2026
Experimental models: Organisms/strains		
Mouse: BALB/c mice	Japan SLC	N/A
Mouse: C.KOR/Stm Slc-Apoe mice	Japan SLC	N/A
Oligonucleotides		
CleanCap Fluc mRNA (5moU)	TriLink BioTechnologies	Cat#L-7202-1000
sgRNA sequence: sgTTR-G211: mU*mU*mA*CAGCCA CGUCUACAGCAGUUUUAGAGCUAGAAAUAGCAAGU UAAAAUAAGGCUAGUCCGUUAUCAACUUGAAAAAG UGGCACCGAGUCGGUGCmU*mU*mU*U	Integrated DNA Technologies, Inc	N/A

(*Continued on next page*)

Continued

REAGENT or RESOURCE	SOURCE	IDENTIFIER
sgRNA sequence: sgF9-5: mG*mA*mA*GCACCUGAAC ACCGUCAGUUUUAGAGCUAGAAAUAGCAAGUUAAA AUAAGGCUAGUCCGUUAUCAACUUGAAAAAGUG GCACCGAGUCGGUGCmU*mU*mU*U	Integrated DNA Technologies, Inc	N/A
sgRNA sequence: sgAT-1: mU*mG*mU*GCAUUUACC GCUCCCCUGUUUUAGAGCUAGAAAUAGCAAGUUA AAAUAAGGCUAGUCCGUUAUCAACUUGAAAAAGU GGCACCGAGUCGGUGCmU*mU*mU*U	Integrated DNA Technologies, Inc	N/A
sgRNA sequence: sgGFP10#2: mC*mU*mC*GUGACCA CCCUGACCUAGUUUUAGAGCUAGAAAUAGCAAGUU AAAAUAAGGCUAGUCCGUUAUCAACUUGAAAAAGU GGCACCGAGUCGGUGCmU*mU*mU*U	Integrated DNA Technologies, Inc	N/A
Software and algorithms		
GraphPad Prism software version 10.1.2	GraphPad Software	N/A
Other		
qEV ORIGINAL gen 2 smart column 35 nm	IZON	Cat#ICO-135
RPMI-1640 with L-Glutamine and Phenol Red	Wako	Cat#189-02025

EXPERIMENTAL MODEL AND STUDY PARTICIPANT DETAILS

Animals

The experimental protocols were all reviewed and approved by the Hokkaido University Animal Care Committee under the guidelines for the care and use of laboratory animals (approval number: 20-0176). BALB/c mice (female, 4 weeks old) and C.KOR/Stm Slc-Apoe mice (female, 4 weeks old) were sourced from Japan SLC (Shizuoka, Japan). Mice were maintained on a regular 12-h light/12-h dark cycle in a specific animal facility at Hokkaido University. Four to five mice were housed in each cage. The mice were fed a pelleted mouse diet (cat# 5053, LabDiet, USA) and were provided water *ad libitum*.

Cells

Hepa1c1c7 cells were perchased from ATCC (). Cells were thawed from frozen stock in 1.5 mL cryo-tube, dilued in 10 mL of RPMI-1640 supplemented with 10% heat-inactivated FBS and centrifuged to remove any traces of the cryoprotectant. Then, the cells were incubated in 10-cm dish (TC treated; Nunc, Thermo Scientific) containing 10 mL of RPMI-1640 supplemented with 10% heat-inactivated FBS at 37°C and 5% CO_2. Once cells reached 90% confluence, cell cultures were passed to a new10-cm dish using 0.05% Trypsin-EDTA followed by centrifugation and resuspension in 10 mL of fresh RPMI-1640 supplemented with 10% heat-inactivated FBS and subsequent incubation at 37°C and 5% CO_2. No mycoplasma contamination was confirmed by DNA staining with Hoechst33342 (Dojindo, Kumamoto, Japan).

METHOD DETAILS

The pH-sensitive cationic lipids CL4H6 and CL4F6 were synthesized as previously described.[20,21] The chol and 6-(p-toluidino)-2-naphthalenesulfonic acid sodium salt (TNS) were purchased from SIGMA Aldrich (St. Louis, MO, USA). The 1,2-distearoyl-*sn*-glycero-3-phosphocholine (DSPC) and 2-dimirystoyl-*rac*-glycero, methoxyethyleneglycol 2000 ether (PEG-DMG) were obtained from the NOF Corporation (Tokyo, Japan). DLin-MC3-DMA (MC3) was obtained from Selleck Biotech (Tokyo, Japan). SM-102 was purchased from Cayman Chemical (Ann Arbor, MI, USA). ALC-0315 was obtained from Ambeed, Inc. (Arlington Hts, IL, USA). Firefly luciferase (Fluc)-encoding mRNA (CleanCap, 5moU modified) was purchased from Trilink BioTechnologies (San Diego, CA, USA). Recombinant spCas9 nuclease (TrueCut Cas9 protein v2), 1,1′-dioctadecyl-3,3,3′,3′-tetramethylindodicarbocyanine, 4-chlorobenzenesulfonate salt (DiD), 1,1′-dioctadecyl-3,3,3′,3′-tetramethylindotricarbocyanine iodide (DiR), and Ribogreen were purchased from Thermo Fisher Scientific (MA, USA). Single-guide RNA (sgRNA) and single-stranded oligodeoxynucleotides (ssODNs) were purchased from Integrated DNA Technologies, Inc. (Coralville, IA, USA) (Tables S1 and S2). Coagulation factor 7 (F7)-targeting siRNA (siF7) was purchased from Hokkaido System Science Co. Ltd. (Sapporo, Japan). The siF7 sense and antisense strand sequences were 5′-GGA ucA ucu cAA Guc uuA cTsT-3′ and 5′-GuA AGA cuu GAG AuG Auc cTsT-3′, respectively. The 2′-Fluoro-modified nucleotides are represented in the lower case, and the phosphorothioate linkage is represented as s. An iLiNP microfluidic device[51] was kindly provided by M. Tokeshi and M. Maeki (Hokkaido University, Hokkaido, Japan). Human recombinant ApoE3 protein albumin from bovine serum (fraction V, pH7.0) was purchased from Wako Chemical (Osaka, Japan).

Experimental section

General information for lipid synthesis

^{1}H NMR spectra were obtained using either a JEOL ECZ500R or ECZ400 instrument with tetramethyl silane as the internal standard (0 ppm). All reactions were monitored via thin-layer chromatography (TLC) on pre-coated TLC plates (Millipore) visualized via UV light (254 nm), phosphomolybdic acid stain, *p*-anisaldehyde stain, ninhydrin stain, or bromocresol green stain. The products were purified using a Biotage Selekt system equipped with an ELSD detector. The final products were analyzed using a compact mass spectrometer (Expression CMS; Advion Interchim Scientific Inc., NY, USA) equipped with a Plate Express automated TLC plate reader (Advion Interchim Scientific). The purity of the final products was analyzed using an LCMS-2050 (Shimazu Corporation) with an ELSD-LT III detector (Shimazu Corporation). Separation was carried out using a Shim-pack Arata C18 Column (pore size: 120 Å, particle size: 5 μm, inner diameter: 50 mm, length: 2.0 mm) and a gradient of 60–98% isopropanol/acetonitrile (2:1) in water with 5 mM ammonium acetate over 8 min and held at 98% isopropanol/acetonitrile (2:1) with 5 mM ammonium acetate for 1 min at 0.2 mL/min. For ionizable lipids with a higher carbon number (CL4F10_β-7, CL4F11_β-8, CL4F17_β, and CL4F12_ε-6), 0.1% formic acid was added to both mobile phases instead of 5 mM ammonium acetate to appropriately adjust the retention time. The injection volume was 1 μL and the column temperature was 60°C. All general reagents were purchased from commercial sources and were used without further purification.

Synthesis of 7-(4-(dipropylamino)butyl)-7-hydroxy-13-((3-propylhexanoyl)oxy)tridecyl 3-ethylheptanoate (CL4F 6_β-3)

Synthesis of ethyl 3-propylhex-2-enoate

NaH (60% in mineral oil, 0.40 g, 10.0 mmol) was added to triethyl phosphonoacetate (2.1 mL, 10.5 mmol) dissolved in THF (20 mL). The reaction mixture was stirred on ice for 30 min. Then, 4-Heptanone (0.57 g, 5.0 mmol) was added to the reaction mixture. The reaction mixture was stirred at 65°C overnight. The reaction mixture was cooled to room temperature, diluted with EtOAc and was washed with water and brine, and dried over anhydrous Na_2SO_4. The solution was filtered, and the filtrate was evaporated. This gave 1.76 g (191%) of ethyl 3-propylhex-2-enoate as a yellow oil. The crude product was used for the next reaction without further purification.

Synthesis of ethyl 3-propylhexanoate

Ethyl 3-propylhex-2-enoate (1.76 g) was dissolved in a mixture of MeOH (10 mL) and DCM (10 mL) under an Ar atmosphere. Pd/C (176 mg, 10 wt %) was added. The mixture was hydrogenated under balloon pressure at ambient temperature overnight. The reaction mixture was filtered through a small pad of celite, and washed with DCM. The filtrate was evaporated. The residue was loaded onto a normal-phase column (Sfär Silica HC D, Biotage) and purified by flash chromatography (Selekt, Biotage) with a gradient mobile phase of hexane and EtOAc. This gave 0.59 g (63%) of ethyl 3-propylhexanoate as a colorless oil.

Synthesis of 3-propylhexanoic acid

Ethyl 3-propylhexanoate (0.59 g) was dissolved in a mixture of 2-propanol (10.7 mL) and water (5.3 mL). KOH (1.77 g, 31.5 mmol) was added, and the reaction mixture was stirred at 70°C overnight. The reaction mixture was cooled to room temperature. Hexane was added and the mixture was washed with 1 N HCl aq., water, and brine, and dried over anhydrous Na_2SO_4. The solution was filtered, and the filtrate was evaporated. This gave 0.46 g (92%) of 3-propylhexanoic acid as a colorless oil. The crude product was used for the next reaction without further purification.

Synthesis of 7-(4-(dipropylamino)butyl)-7-hydroxy-13-((3-propylhexanoyl)oxy)tridecyl 3-ethylheptanoate

3-Propylhexanoic acid (348 mg, 2.2 mmol) was dissolved in anhydrous DCM (10 mL) and 7-(4-dipropylamino)butyl)tridecane-1,7,13-triol (388 mg, 1.0 mmol); DMAP (12.2 mg, 0.10 mmol) and EDCI-HCl (479 mg, 2.5 mmol) were added to the mixture. The reaction mixture was evaporated after being stirred at ambient temperature overnight. The residue was suspended with EtOAc, washed with 0.5 N NaOH aq. and brine, and dried over anhydrous Na_2SO_4. The solution was filtered, and the filtrate was evaporated. The residue was loaded onto a reverse-phase column (HP C18Aq, Teledyne ISCO), and purified by flash chromatography (CombiFlash Rf, Teledyne ISCO) using a gradient mobile phase of water with 0.1% TFA and acetonitrile/2-propanol (1:1) and 0.1% TFA. This gave 340 mg (52%) of 7-(4-(dipropylamino)butyl)-7-hydroxy-13-((3-propylhexanoyl)oxy)tridecyl 3-ethylheptanoate (CL4F 6_β-3) as a colorless oil.

Synthesis of 7-(4-(dipropylamino)butyl)-7-hydroxytridecane-1,13-diyl bis(3-butylheptanoate) (CL4F 7_β-4)

Synthesis of ethyl 3-butylhept-2-enoate

NaH (60% in mineral oil, 0.40 g, 10.0 mmol) was added to triethyl phosphonoacetate (2.1 mL, 10.5 mmol) and the mixture was dissolved in THF (20 mL). The reaction mixture was stirred on ice for 30 min. Then, 5-nonanone (0.71 g, 5.0 mmol) was added to the reaction mixture. The reaction mixture was stirred at 65°C overnight. The reaction mixture was cooled to room temperature, diluted with EtOAc, washed with water and brine, and dried over anhydrous Na_2SO_4. The solution was filtered, and the filtrate was evaporated. This gave 1.65 g (155%) of ethyl 3-butylhept-2-enoate as a yellow oil. The crude product was used for the next reaction without further purification.

Synthesis of ethyl 3-butylheptanoate

Ethyl 3-butylhept-2-enoate (1.65 g) was dissolved in a mixture of MeOH (10 mL) and DCM (10 mL), and degassed with argon. Pd/C (165 mg, 10 wt %) was added. The mixture was hydrogenated under balloon pressure at ambient temperature overnight. The reaction mixture was filtered through a small pad of celite, and washed with DCM. The filtrate was evaporated. The residue was loaded onto a normal-phase column (Sfär Silica HC D, Biotage), and purified by flash chromatography (Selekt, Biotage) with a gradient mobile phase of hexane and EtOAc. This gave 0.50 g (47%) of ethyl 3-butylheptanoate as a colorless oil.

Synthesis of 3-butylheptanoic acid

Ethyl 3-butylheptanoate (0.54 g) was dissolved in a mixture of 2-propanol (7.8 mL) and water (3.9 mL). KOH (1.29 g, 23 mmol) was added, and the reaction mixture was stirred at 70°C overnight. The reaction mixture was cooled to room temperature, hexane was added and the mixture was washed with 1 N HCl aq., water, and brine, and dried over anhydrous Na_2SO_4. The solution was filtered, and the filtrate was evaporated. This gave 0.41 g (95%) of 3-butylheptanoic acid as a colorless oil. The crude product was used for the next reaction without further purification.

Synthesis of 7-(4-(dipropylamino)butyl)-7-hydroxytridecane-1,13-diyl bis(3-butylheptanoate)

3-Butylheptanoic acid (261 mg, 1.4 mmol) was dissolved in anhydrous DCM (10 mL) and 7-(4-dipropylamino)butyl)tridecane-1,7,13-triol (247 mg, 0.64 mmol); DMAP (7.8 mg, 0.064 mmol) and EDCI-HCl (307 mg, 1.6 mmol) were added to the mixture. The reaction mixture was evaporated after being stirred overnight at ambient temperature. The residue was suspended with EtOAc, washed with 0.5 N NaOH aq. and brine, and dried over anhydrous Na_2SO_4. The solution was filtered, and the filtrate was evaporated. The residue was loaded onto a reverse-phase column (HP C18Aq, Teledyne ISCO), and purified by flash chromatography (CombiFlash Rf, Teledyne ISCO) with a gradient mobile phase of water with 0.1% TFA and acetonitrile/2-propanol (1:1) with 0.1% TFA. This gave 150 mg (32%) of 7-(4-(dipropylamino) butyl)-7-hydroxytridecane-1,13-diyl bis(3-butylheptanoate) (CL4F 7_β-4) as a colorless oil.

Synthesis of 7-(4-(dipropylamino)butyl)-7-hydroxytridecane-1,13-diyl bis(3-pentyloctanoate) (CL4F 8_β-5)

Synthesis of ethyl 3-pentyloct-2-enoate

NaH (60% in mineral oil, 0.40 g, 10.0 mmol) was added to triethyl phosphonoacetate (2.1 mL, 10.5 mmol) and the mixture was dissolved in THF (20 mL). The reaction mixture was stirred on ice for 30 min. Then, 6-undecanone (0.85 g, 5.0 mmol) was added to the reaction mixture. The reaction mixture was stirred at 65°C overnight. The reaction mixture was cooled to room temperature, diluted with EtOAc, washed with water and brine, and dried over anhydrous Na_2SO_4. The solution was filtered, and the filtrate was evaporated. This gave 3.94 g (164%) of ethyl 3-pentyloct-2-enoate as a yellow oil. The crude product was used for the next reaction without further purification.

Synthesis of ethyl 3-pentyloctanoate

Ethyl 3-pentyloct-2-enoate (1.65 g) was dissolved in a mixture of MeOH (10 mL) and DCM (10 mL) under an Ar atmosphere. Pd/C (394 mg, 10 wt %) was added. The mixture was hydrogenated under balloon pressure at ambient temperature overnight. The reaction mixture was filtered through a small pad of celite, and washed with DCM. The filtrate was evaporated. The residue was loaded onto a normal-phase column (Sfär Silica HC D, Biotage), and purified by flash chromatography (Selekt, Biotage) with a gradient mobile phase of hexane and EtOAc. This gave 1.11 g (46%) of ethyl 3-pentyloctanoate as a colorless oil.

Synthesis of 3-pentyloctanoic acid

Ethyl 3-pentyloctanoate (1.11 g) was dissolved in a mixture of 2-propanol (15.6 mL) and water (7.8 mL). KOH (2.58 g, 46 mmol) was added, and the reaction mixture was stirred at 70°C overnight. The reaction mixture was cooled to room temperature, hexane was added, and the mixture was washed with 1 N HCl aq., water, and brine, and dried over anhydrous Na_2SO_4. The solution was filtered, and the filtrate was evaporated. This gave 0.94 g (97%) of 3-pentyloctanoic acid as a colorless oil. The crude product was used for the next reaction without further purification.

Synthesis of 7-(4-(dipropylamino)butyl)-7-hydroxytridecane-1,13-diyl bis(3-pentyloctanoate)

3-Pentyloctanoic acid (461 mg, 2.15 mmol) was dissolved in anhydrous DCM (10 mL) and 7-(4-dipropylamino)butyl)tridecane-1,7,13-triol (379 mg, 0.98 mmol); DMAP (11.9 mg, 0.10 mmol) and EDCI-HCl (469 mg, 2.45 mmol) were added to the mixture. The reaction mixture was evaporated after being stirred at ambient temperature overnight. The residue was suspended with EtOAc, washed with 0.5 N NaOH aq. and brine, and dried over anhydrous Na_2SO_4. The solution was filtered, and the filtrate was evaporated. The residue was loaded onto a reverse-phase column (HP C18Aq, Teledyne ISCO), and purified by flash chromatography (CombiFlash Rf, Teledyne ISCO) with a gradient mobile phase of water with 0.1% TFA and acetonitrile/2-propanol (1:1) with 0.1% TFA. This gave 320 mg (42%) of 7-(4-(dipropylamino)butyl)-7-hydroxytridecane-1,13-diyl bis(3-pentyloctanoate) (CL4F 8_β-5) as a yellow oil.

Synthesis of 7-(4-(dipropylamino)butyl)-7-hydroxytridecane-1,13-diyl bis(3-hexylnonanoate) (CL4F 9_β-6)

Synthesis of ethyl 3-hexylnon-2-enoate

NaH (60% in mineral oil, 0.40 g, 10.0 mmol) was added to triethyl phosphonoacetate (2.1 mL, 10.5 mmol) and dissolved in THF (20 mL). The reaction mixture was stirred on ice for 30 min. Then, 9-tridecanone (0.99 g, 5.0 mmol) was added to the reaction mixture. The reaction mixture was stirred at 65°C overnight. The reaction mixture was cooled to room temperature, diluted with EtOAc, washed with water and brine, and dried over anhydrous Na_2SO_4. The solution was filtered, and the filtrate was evaporated. This gave 1.63 g (121%) of ethyl 3-hexylnon-2-enoate as a colorless oil. The crude product was used for the next reaction without further purification.

Synthesis of ethyl 3-hexylnonanoate

Ethyl 3-hexylnon-2-enoate (1.63 g) was dissolved in a mixture of MeOH (10 mL) and DCM (10 mL) under an Ar atmosphere. Pd/C (163 mg, 10 wt %) was added. The mixture was hydrogenated under balloon pressure at ambient temperature overnight. The reaction mixture was filtered through a small pad of celite, and washed with DCM. The filtrate was evaporated. The residue was loaded onto a normal-phase column (Sfär Silica HC D, Biotage), and purified by flash chromatography (Selekt, Biotage) with a gradient mobile phase of hexane and EtOAc. This gave 0.54 g (40%) of ethyl 3-hexylnonanoate as a colorless oil.

Synthesis of 3-hexylnonanoic acid

Ethyl 3-octylundecanoate (0.54 g) was dissolved in a mixture of 2-propanol (6.8 mL) and water (3.4 mL). KOH (1.12 g, 20 mmol) was added, and the reaction mixture was stirred at 70°C overnight. The reaction mixture was cooled to room temperature, hexane was added and the mixture was washed with 1 N HCl aq., water, and brine, and dried over anhydrous Na_2SO_4. The solution was filtered, and the filtrate was evaporated. This gave 0.44 g (92%) of 3-hexylnonanoic acid as a colorless oil. The crude product was used for the next reaction without further purification.

Synthesis of 7-(4-(dipropylamino)butyl)-7-hydroxytridecane-1,13-diyl bis(3-hexylnonanoate)

3-Hexylnonanoic acid (339 mg, 1.4 mmol) was dissolved in anhydrous DCM (10 mL) and 7-(4-dipropylamino)butyl)tridecane-1,7,13-triol (247 mg, 0.64 mmol); DMAP (7.8 mg, 0.064 mmol) and EDCI-HCl (307 mg, 1.6 mmol) were added to the mixture. The reaction mixture was evaporated by being stirred at ambient temperature overnight. The residue was suspended with EtOAc, washed with 0.5 N NaOH aq. and brine, and dried over anhydrous Na_2SO_4. The solution was filtered, and the filtrate was evaporated. The residue was loaded onto a reverse-phase column (HP C18Aq, Teledyne ISCO), and purified by flash chromatography (CombiFlash Rf, Teledyne ISCO) with a gradient mobile phase of water with 0.1% TFA and acetonitrile/2-propanol (1:1) with 0.1% TFA. This gave 250 mg (46%) of 7-(4-(dipropylamino) butyl)-7-hydroxytridecane-1,13-diyl bis(3-hexylnonanoate) (CL4F 9_β-6) as a colorless oil.

Synthesis of 7-(4-(dipropylamino)butyl)-7-hydroxytridecane-1,13-diyl bis(3-heptyldecanoate) (CL4F 10_β-7)

Synthesis of ethyl 3-heptyldec-2-enoate

NaH (60% in mineral oil, 0.22 g, 5.5 mmol) was added to triethyl phosphonoacetate (1.20 mL, 6.0 mmol) and dissolved in tetrahydrofurane (THF) (20 mL). The reaction mixture was stirred on ice for 3 h. 8-Pentadecanone (1.13g, 5.0 mmol) was added to the reaction mixture. The reaction mixture was then refluxed overnight. The reaction mixture was cooled to room temperature, diluted with ethyl acetate (EtOAc) and was washed with water and brine, and dried over anhydrous Na_2SO_4. The solution was filtered, and the filtrate was evaporated. This gave 1.63 g (110%) of a mixture of 8-pentadecanone and ethyl 3-heptyldec-2-enoate as a yellow oil. The crude product was used for the next reaction without further purification.

Synthesis of ethyl 3-heptyldecanoate

Ethyl 3-heptyldec-2-enoate (1.63 g) was dissolved in a mixture of methanol (MeOH) (10 mL) and dichloromethane (DCM) (10 mL) under an Ar atmosphere. Pd/C (163 mg, 10 wt %) was added. The mixture was hydrogenated under balloon pressure at ambient temperature overnight. The reaction mixture was filtered through a small pad of celite, and washed with DCM. The filtrate was evaporated. The residue was loaded onto a normal-phase column (Sfär Silica HC D, Biotage), and purified by flash chromatography (Selekt, Biotage) to realize a gradient mobile phase of hexane and EtOAc. This gave 1.16 g (45%) of a mixture of 8-pentadecanone and ethyl 3-heptyldecanoate as a colorless oil.

Synthesis of 3-heptyldecanoic acid

A mixture of 8-pentadecanone and ethyl 3-heptyldecanoate (1.16 g) was dissolved in a mixture of 2-propanol (15.3 mL) and water (7.7 mL). KOH (1.54 g, 27.4 mmol) was added, and the reaction mixture was stirred at 70°C overnight. The reaction mixture was cooled to room temperature, hexane was added and the mixture was washed with 1 N HCl aq., water, and brine, and dried over anhydrous Na_2SO_4. The solution was filtered, and the filtrate was evaporated. This gave 1.05 g (97%) of a mixture of 8-pentadecanone and 3-heptyldecanoic acid as a colorless oil. The crude product was used for the next reaction without further purification.

Synthesis of 7-(4-(dipropylamino)butyl)-7-hydroxytridecane-1,13-diyl bis(3-heptyldecanoate)

A mixture of 8-pentadecanone and 3-heptyldecanoic acid (1.05 g, 2.20 mmol of 3-heptyldecanoic acid) was dissolved in anhydrous DCM (10 mL) and 7-(4-dipropylamino)butyl)tridecane-1,7,13-triol (388 mg, 1.0 mmol); DMAP (12.2 mg, 0.1 mmol) and EDCI-HCl (479 mg, 2.5 mmol) were added to the mixture. The reaction mixture was evaporated after being stirred at ambient temperature overnight. The residue was suspended with EtOAc, washed with 0.5 N NaOH aq. and brine, and dried over anhydrous Na_2SO_4. The solution was filtered, and the filtrate was evaporated. The residue was loaded onto a reverse-phase column (HP C18Aq, Teledyne ISCO), and purified by flash chromatography (CombiFlash Rf, Teledyne ISCO) with a gradient mobile phase of water with 0.1% TFA and acetonitrile/2-propanol (1:1) with 0.1% TFA. This gave 360 mg (40%) of 7-(4-(dipropylamino)butyl)-7-hydroxytridecane-1,13-diyl bis(3-heptyldecanoate) (CL4F 10_β-7) as a colorless oil.

Synthesis of 7-(4-(dipropylamino)butyl)-7-hydroxytridecane-1,13-diyl bis(3-octylundecanoate) (CL4F 11_β-8)

Synthesis of ethyl 3-octylundec-2-enoate

NaH (60% in mineral oil, 0.40 g, 10.0 mmol) was added to triethyl phosphonoacetate (2.1 mL, 10.5 mmol) and dissolved in THF (20 mL). The reaction mixture was stirred on ice for 30 min. Then, 9-heptadecanone (1.27 g, 5.0 mmol) was added to the reaction mixture. The reaction mixture was stirred at 65°C overnight. The reaction mixture was cooled to room temperature, diluted with EtOAc, washed with water and brine, and dried over anhydrous Na_2SO_4. The solution was filtered, and the filtrate was evaporated. This gave 2.12 g (131%) of ethyl 3-octylundec-2-enoate as a reddish brown oil. The crude product was used for the next reaction without further purification.

Synthesis of ethyl 3-octylundecanoate

Ethyl 3-octylundec-2-enoate (2.12 g) was dissolved in a mixture of MeOH (10 mL) and DCM (10 mL) under an Ar atmosphere. Pd/C (212 mg, 10 wt %) was added. The mixture was hydrogenated under balloon pressure at ambient temperature overnight. The reaction mixture was filtered through a small pad of celite, and washed with DCM. The filtrate was evaporated. The residue was loaded onto a normal-phase column (Sfär Silica HC D, Biotage), and purified by flash chromatography (Selekt, Biotage) with a gradient mobile phase of hexane and EtOAc. This gave 1.05 g (64%) of ethyl 3-octylundecanoate as a colorless oil.

Synthesis of 3-octylundecanoic acid

Ethyl 3-octylundecanoate (1.05 g) was dissolved in a mixture of 2-propanol (10.8 mL) and water (5.4 mL). KOH (1.79 g, 32 mmol) was added, and the reaction mixture was stirred at 70°C overnight. The reaction mixture was cooled to room temperature, hexane was added and the mixture was washed with 1 N HCl aq., water, and brine, and dried over anhydrous Na_2SO_4. The solution was filtered, and the filtrate was evaporated. This gave 0.84 g (88%) of 3-octylundecanoic acid as a yellow oil. The crude product was used for the next reaction without further purification.

Synthesis of 7-(4-(dipropylamino)butyl)-7-hydroxytridecane-1,13-diyl bis(3-octylundecanoate)

3-Octylundecanoic acid (418 mg, 1.4 mmol) was dissolved in anhydrous DCM (10 mL) and 7-(4-dipropylamino)butyl)tridecane-1,7,13-triol (247 mg, 0.64 mmol); DMAP (7.8 mg, 0.064 mmol) and EDCI-HCl (307 mg, 1.6 mmol) were added to the mixture. The reaction mixture was evaporated after being stirred at ambient temperature overnight. The residue was suspended with EtOAc, washed with 0.5 N NaOH aq. and brine, and dried over anhydrous Na_2SO_4. The solution was filtered, and the filtrate was evaporated. The residue was loaded onto a reverse-phase column (HP C18Aq, Teledyne ISCO), and purified by flash chromatography (CombiFlash Rf, Teledyne ISCO) with a gradient mobile phase of water with 0.1% TFA and acetonitrile/2-propanol (1:1) with 0.1% TFA. This gave 384 mg (63%) of 7-(4-(dipropylamino) butyl)-7-hydroxytridecane-1,13-diyl bis(3-octylundecanoate) (CL4F 11_β-8) as a yellow oil.

Synthesis of 7-(4-(dipropylamino)butyl)-7-hydroxytridecane-1,13-diyl bis(2-cycloheptylacetate) (CL4F 9_β)

Synthesis of ethyl 2-cycloheptylideneacetate

NaH (60% in mineral oil, 0.40 g, 10.0 mmol) was added to triethyl phosphonoacetate (2.1 mL, 10.5 mmol) and dissolved in THF (20 mL). The reaction mixture was stirred on ice for 30 min. Cycloheptanone (0.56 g, 5.0 mmol) was added to the reaction mixture. The reaction mixture was stirred at 65°C overnight. The reaction mixture was cooled to room temperature, diluted with EtOAc and was washed with water and brine, and dried over anhydrous Na_2SO_4. The solution was filtered, and the filtrate was evaporated. This gave 1.72 g (189%) of ethyl 2-cycloheptylideneacetate as a colorless oil. The crude product was used for the next reaction without further purification.

Synthesis of ethyl 2-cycloheptylacetate

Ethyl 2-cycloheptylideneacetate (1.72 g) was dissolved in a mixture of MeOH (10 mL) and DCM (10 mL) under an Ar atmosphere. Pd/C (172 mg, 10 wt %) was added. The mixture was hydrogenated under balloon pressure at ambient temperature overnight. The reaction mixture was filtered through a small pad of celite, and washed with DCM. The filtrate was evaporated. The residue was loaded onto a normal-phase column (Sfär Silica HC D, Biotage), and purified by flash chromatography (Selekt, Biotage) with a gradient mobile phase of hexane and EtOAc. This gave 0.80 g (87%) of ethyl 2-cycloheptylacetate as a colorless oil.

Synthesis of 2-cycloheptylacetic acid

Ethyl 2-cycloheptylacetate (0.80 g) was dissolved in a mixture of 2-propanol (14.8 mL) and water (7.4 mL). KOH (2.45 g, 43.7 mmol) was added, and the reaction mixture was stirred at 70°C overnight. The reaction mixture was cooled to room temperature, hexane was added and the mixture was washed with 1 N HCl aq., water, and brine, and dried over anhydrous Na_2SO_4. The solution was filtered, and the filtrate was evaporated. This gave 0.60 g (77%) of 2-cycloheptylacetic acid as a colorless oil. The crude product was used for the next reaction without further purification.

Synthesis of -(4-(dipropylamino)butyl)-7-hydroxytridecane-1,13-diyl bis(2-cycloheptylacetate)

2-Cycloheptylacetic acid (600 mg, 3.8 mmol) was dissolved in anhydrous DCM (10 mL) and 7-(4-dipropylamino)butyl)tridecane-1,7,13-triol (670 mg, 1.73 mmol); DMAP (21 mg, 0.10 mmol) and EDCI-HCl (830 mg, 2.5 mmol) were added to the mixture. The reaction mixture was stirred at ambient temperature overnight. The reaction mixture was evaporated. The residue was suspended with EtOAc, washed with 0.5 N NaOH aq. and brine, and dried over anhydrous Na_2SO_4. The solution was filtered, and the filtrate was evaporated. The residue was loaded onto a reverse-phase column (HP C18Aq, Teledyne ISCO), and purified by flash chromatography (CombiFlash Rf, Teledyne ISCO) with a gradient mobile phase of water with 0.1% TFA and acetonitrile/2-propanol (1:1) with 0.1% TFA. This gave 430 mg (27%) of 7-(4-(dipropylamino) butyl)-7-hydroxytridecane-1,13-diyl bis(2-cycloheptylacetate) (CL4F 9_β) as a colorless oil.

Synthesis of 7-(4-(dipropylamino)butyl)-7-hydroxytridecane-1,13-diyl bis(2-cyclododecylacetate) (CL4F 14_β)

Synthesis of ethyl 2-cyclododecylideneacetate

NaH (60% in mineral oil, 0.40 g, 10.0 mmol) was added to triethyl phosphonoacetate (2.1 mL, 10.5 mmol) and dissolved in THF (20 mL). The reaction mixture was stirred on ice for 30 min. Cyclododecanone (0.91 g, 5.0 mmol) was added to the reaction mixture. The reaction mixture was stirred at 65°C overnight. The reaction mixture was cooled to room temperature, diluted with EtOAc, washed with water and brine, and dried over anhydrous Na_2SO_4. The solution was filtered, and the filtrate was evaporated. This gave 2.0 g (162%) of ethyl 2-cyclododecylideneacetate as a yellow oil. The crude product was used for the next reaction without further purification.

Synthesis of ethyl 2-cyclododecylacetate

Ethyl 2-cyclododecylideneacetate (2.0 g) was dissolved in a mixture of MeOH (10 mL) and DCM (10 mL), and degassed with argon. Pd/C (200 mg, 10 wt %) was added. The mixture was hydrogenated under balloon pressure at ambient temperature overnight. The reaction mixture was filtered through a small pad of celite, and washed with DCM. The filtrate was evaporated. The residue was loaded onto a normal-phase column (Sfär Silica HC D, Biotage), and purified by flash chromatography (Selekt, Biotage) with a gradient mobile phase of hexane and EtOAc. This gave 1.06 g (84%) of ethyl 2-cyclododecylacetate as a colorless oil.

Synthesis of 2-cyclododecylacetic acid

Ethyl 2-cyclododecylacetate (1.06 g) was dissolved in a mixture of 2-propanol (14.1 mL) and water (7.1 mL). KOH (2.35 g, 41.8 mmol) was added, and the reaction mixture was stirred at 70°C overnight. The reaction mixture was cooled to room temperature, hexane was added and the mixture was washed with 1 N HCl aq., water, and brine, and dried over anhydrous Na_2SO_4. The solution was filtered, and the filtrate was evaporated. This gave 0.92 g (82%) of 2-cyclododecylacetic acid as a white solid. The crude product was used for the next reaction without further purification.

Synthesis of 7-(4-(dipropylamino)butyl)-7-hydroxytridecane-1,13-diyl bis(2-cyclododecylacetate)

2-Cyclododecylacetic acid (920 mg, 4.1 mmol) was dissolved in anhydrous DCM (10 mL) and 7-(4-dipropylamino)butyl)tridecane-1,7,13-triol (720 mg, 1.86 mmol); DMAP (23 mg, 0.18 mmol) and EDCI-HCl (890 mg, 4.66 mmol) were added to the mixture. The reaction mixture was evaporated after being stirred at ambient temperature overnight. The residue was suspended with EtOAc, washed with 0.5 N NaOH aq. and brine, and dried over anhydrous Na_2SO_4. The solution was filtered, and the filtrate was evaporated. The residue was loaded onto a reverse-phase column (HP C18Aq, Teledyne ISCO), and purified by flash chromatography (CombiFlash Rf, Teledyne ISCO) with a gradient mobile phase of water with 0.1% TFA and acetonitrile/2-propanol (1:1) with 0.1% TFA. This gave 770 mg (52%) of 7-(4-(dipropylamino) butyl)-7-hydroxytridecane-1,13-diyl bis(2-cyclododecylacetate) (CL4F 14_β) as a colorless oil.

Synthesis of 7-(4-(dipropylamino)butyl)-7-hydroxytridecane-1,13-diyl bis(2-cyclopentadecylacetate) (CL4F 17_β)

Synthesis of ethyl 2-cyclopentadecylideneacetate

NaH (60% in mineral oil, 0.40 g, 10.0 mmol) was added to triethyl phosphonoacetate (2.1 mL, 10.5 mmol) dissolved in THF (20 mL). The reaction mixture was stirred on ice for 30 min. Cyclopentadecanone (1.12 g, 5.0 mmol) was added to the reaction mixture. The reaction mixture was stirred at 65°C overnight. The reaction mixture was cooled to room temperature, diluted with EtOAc, washed with water and brine, and dried over anhydrous Na_2SO_4. The solution was filtered, and the filtrate was evaporated. This gave 2.3 g (156%) of ethyl 2-cyclopentadecylideneacetate as a yellow oil. The crude product was used for the next reaction without further purification.

Synthesis of ethyl 2-cyclopentadecylacetate

Ethyl 2-cyclopentadecylideneacetate (2.3 g) was dissolved in a mixture of MeOH (10 mL) and DCM (10 mL) under an Ar atmosphere. Pd/C (230 mg, 10 wt %) was added. The mixture was hydrogenated under balloon pressure at ambient temperature overnight. The reaction mixture was filtered through a small pad of celite, and washed with DCM. The filtrate was evaporated. The residue was loaded onto a normal-phase column (Sfär Silica HC D, Biotage), and purified by flash chromatography (Selekt, Biotage) with a gradient mobile phase of hexane and EtOAc. This gave 0.84 g (57%) of ethyl 2-cyclopentadecylacetate as a colorless oil.

Synthesis of 2-cyclopentadecylacetic acid

Ethyl 2-cyclopentadecylacetate (0.84 g) was dissolved in a mixture of 2-propanol (7.5 mL) and water (4.7 mL). KOH (1.57 g, 28 mmol) was added, and the reaction mixture was stirred at 70°C overnight. The reaction mixture was cooled to room temperature, hexane was added and the mixture was washed with 1 N HCl aq., water, and brine, and dried over anhydrous Na_2SO_4. The solution was filtered, and the filtrate was evaporated. This gave 0.69 g (91%) of 2-cyclopentadecylacetic acid as a white solid. The crude product was used for the next reaction without further purification.

Synthesis of 7-(4-(dipropylamino)butyl)-7-hydroxytridecane-1,13-diyl bis(2-cyclopentadecylacetate)

2-Cyclopentadecylacetic acid (690 mg, 2.56 mmol) was dissolved in anhydrous DCM (10 mL) and 7-(4-dipropylamino)butyl)tridecane-1,7,13-triol (450 mg, 1.16 mmol); DMAP (14.2 mg, 0.12 mmol) and EDCI-HCl (560 mg, 2.9 mmol) were added to the mixture. The reaction mixture was evaporated after being stirred at ambient temperature overnight. The residue was suspended with EtOAc, washed with 0.5 N NaOH aq. and brine, and dried over anhydrous Na_2SO_4. The solution was filtered, and the filtrate was evaporated. The residue was loaded onto a reverse-phase column (HP C18Aq, Teledyne ISCO), and purified by flash chromatography (CombiFlash Rf, Teledyne ISCO) with a gradient mobile phase of water with 0.1% TFA and acetonitrile/2-propanol (1:1) with 0.1% TFA. This gave 280 mg (27%) of 7-(4-(dipropylamino)butyl)-7-hydroxytridecane-1,13-diyl bis(2-cyclopentadecylacetate) (CL4F 17_β) as a colorless oil.

Synthesis of 7-(4-(dipropylamino)butyl)-7-hydroxytridecane-1,13-diyl bis(6-ethyldecanoate) (CL4F 10_ε-2)

Synthesis of ethyl 6-ethyldec-4-enoate

To a stirred suspension of (4-ethoxy-4-oxobutyl) triphenyl phosphonium bromide (2.74 g, 6.0 mmol) in anhydrous THF (6 mL) under an Ar atmosphere cooled to 0°C was added potassium *tert*-butoxide (1 M solution in THF) (6.0 mL) dropwise. The reaction mixture was stirred at room temperature for 30 min, then 2-ethylhexanal (0.64 g, 5.0 mmol) was added, and the reaction mixture was stirred at room temperature overnight. The reaction mixture was quenched with sat. NH_4Cl aq. and diluted with Et_2O, washed with brine, and dried over with anhydrous Na_2SO_4. The solution was filtered, and the filtrate was evaporated. The residue was dissolved in hexane and through silica gel, and the solution was evaporated. The residue was loaded onto a normal-phase column (Sfär Silica HC D, Biotage), and purified by flash chromatography (Selekt, Biotage) with a gradient mobile phase of hexane and EtOAc. This gave 0.38 g (34%) of ethyl 6-ethyldec-4-enoate as a colorless oil.

Synthesis of ethyl 6-ethyldecanoate

Ethyl 6-ethyldec-4-enoate (0.38 g, 1.69 mmol) was dissolved in a mixture of methanol (MeOH) (10 mL) and dichloromethane (DCM) (10 mL) under an Ar atmosphere. Pd/C (38 mg, 10 wt %) was added. The mixture was hydrogenated under balloon pressure at ambient temperature overnight. The reaction mixture was filtered through a small pad of celite, and washed with DCM. The filtrate was evaporated. This gave 0.38 g (99%) of ethyl 6-ethyldecanoate as a colorless oil. The crude product was used for the next reaction without further purification.

Synthesis of 6-ethyldecanoic acid

Ethyl 6-ethyldecanoate (0.38 g, 1.67 mmol) was dissolved in a mixture of 2-propanol (5.6 mL) and water (2.8 mL). KOH (0.94 g, 16.7 mmol) was added, and the reaction mixture was stirred at 70°C overnight. The reaction mixture was cooled to room temperature, hexane was added and the mixture was washed with 1 N HCl solution, water, and brine, and dried over anhydrous Na_2SO_4. The solution was filtered, and the filtrate was evaporated. This gave 0.31 g (90%) of 6-ethyldecanoic acid as a colorless oil. The crude product was used for the next reaction without further purification.

Synthesis of 7-(4-(dipropylamino)butyl)-7-hydroxytridecane-1,13-diyl bis(6-ethyldecanoate)

6-Ethyldecanoic acid (305 g, 1.5 mmol) was dissolved in anhydrous DCM (10 mL) and 7-(4-dipropylamino)butyl)tridecane-1,7,13-triol (264 mg, 0.68 mmol); DMAP (8.3 mg, 0.064 mmol) and EDCI-HCl (326 mg, 1.7 mmol) were added to the mixture. The reaction mixture was evaporated after being stirred at ambient temperature overnight. The residue was suspended with EtOAc, washed with 0.5 N NaOH aq. and brine, and dried over anhydrous Na_2SO_4. The solution was filtered, and the filtrate was evaporated. The residue was loaded onto a reverse-phase column (HP C18Aq, Teledyne ISCO), and purified by flash chromatography (CombiFlash Rf, Teledyne ISCO) with a gradient mobile phase of water with 0.1% TFA and acetonitrile/2-propanol (1:1) with 0.1% TFA. This residue was loaded onto a normal-phase column (Sfär Silica HC D, Biotage), and purified by flash chromatography (Slekt, Biotage) with a gradient mobile phase of DCM and MeOH. This gave 270 mg (52%) of 7-(4-(dipropylamino)butyl)-7-hydroxytridecane-1,13-diyl bis(6-ethyldecanoate) (CL4F 10_ε-2) as a colorless oil.

Synthesis of 7-(4-(dipropylamino)butyl)-7-hydroxytridecane-1,13-diyl bis(6-propylundecanoate) (CL4F 11_ε-3)

Synthesis of 2-propylheptanal

2-Propylheptan-1-ol (1.58 g, 10 mmol) was dissolved in anhydrous DCM (30 mL). TEMPO (15.5 mg, 0.10 mmol) and Bu_4NHSO_4 (0.17 g, 0.50 mmol) were added, and the mixture was cooled on ice. NaOCl-$5H_2O$ (1.98 g, 12.0 mmol) was added, and the reaction mixture was stirred on ice for 3 h. The reaction mixture was quenched with sat. $Na_2S_2O_3$ aq. and diluted with EtOAc and was washed with water and brine and dried over anhydrous Na_2SO_4. The solution was filtered, and the filtrate was evaporated. This gave 1.46 g (93%) of 2-propylheptanal as a colorless oil. The crude product was used for the next reaction without further purification.

Synthesis of ethyl 6-butyldodec-4-enoate

To a stirred suspension of (4-ethoxy-4-oxobutyl) triphenyl phosphonium bromide (5.12 g, 11.2 mmol) in anhydrous THF (8 mL) under an Ar atmosphere cooled to −78°C was added potassium *tert*-butoxide (1 M solution in THF) (11.2 mL) dropwise. The reaction mixture was stirred at −78°C for 30 min, and then 2-propylheptanal (1.46 g) was added. The reaction mixture was gradually warmed to room temperature overnight. The reaction mixture was quenched with sat. NH_4Cl aq. and diluted with Et_2O and was washed with brine and dried over anhydrous Na_2SO_4. The solution was filtered, and the filtrate was evaporated. The residue was dissolved in hexane and through silica gel, and the solution was evaporated. The residue was loaded onto a normal-phase column (Sfär Silica HC D, Biotage), and purified by flash chromatography (Selekt, Biotage) with a gradient mobile phase of hexane and EtOAc. This gave 0.98 g (41%) of ethyl 6-butyldodec-4-enoate as a yellow oil.

Synthesis of ethyl 6-butyldodecanoate

Ethyl 6-butyldodec-4-enoate (0.98 g, 3.85 mmol) was dissolved in a mixture of MeOH (10 mL) and DCM (10 mL) under an Ar atmosphere. Pd/C (98 mg, 10 wt %) was added. The mixture was hydrogenated under balloon pressure at ambient temperature overnight. The reaction mixture was filtered through a small pad of celite, and washed with DCM. The filtrate was evaporated. This gave 0.91 g (92%) of ethyl 6-butyldodecanoate as a cloudy white oil. The crude product was used for the next reaction without further purification.

Synthesis of 6-hexyldodecanoic acid

Ethyl 6-butyldodecanoate (0.91 g, 3.5 mmol) was dissolved in a mixture of 2-propanol (11.8 mL) and water (5.9 mL). KOH (1.96 g, 35 mmol) was added, and the reaction mixture was stirred at 70°C overnight. The reaction mixture was cooled to room temperature, hexane was added and the mixture was washed with 1 N HCl aq., water, and brine, and dried over anhydrous Na_2SO_4. The solution was filtered, and the filtrate was evaporated. This gave 0.78 g (97%) of 6-butyldodecanoic acid as a yellow oil. The crude product was used for the next reaction without further purification.

Synthesis of 7-(4-(dipropylamino)butyl)-7-hydroxytridecane-1,13-diyl bis(6-propylundecanoate)

6-Butyldodecanoic acid (692 mg, 2.7 mmol) was dissolved in anhydrous DCM (10 mL) and 7-(4-dipropylamino)butyl)tridecane-1,7,13-triol (460 mg, 1.2 mmol); DMAP (14.7 mg, 0.12 mmol) and EDCI-HCl (575 mg, 3.0 mmol) were added to the mixture. The reaction mixture was stirred at ambient temperature overnight. The reaction mixture was evaporated. The residue was suspended with EtOAc, washed with 0.5 N NaOH aq. and brine, and dried over anhydrous Na_2SO_4. The solution was filtered, and the filtrate was evaporated. The residue was loaded onto a reverse-phase column (HP C18Aq, Teledyne ISCO), and purified by flash chromatography (CombiFlash Rf, Teledyne ISCO) with a gradient mobile phase of water with 0.1% TFA and acetonitrile/2-propanol (1:1) with 0.1% TFA. This residue was loaded onto a normal-phase column (Sfär Silica HC D, Biotage), and purified by flash chromatography (Slekt, Biotage) with a gradient mobile phase of DCM and MeOH. This gave 445 mg (46%) of 7-(4-(dipropylamino)butyl)-7-hydroxytridecane-1,13-diyl bis(6-propylundecanoate) (CL4F 11_ε-3) as a colorless oil.

Synthesis of 7-(4-(dipropylamino)butyl)-7-hydroxytridecane-1,13-diyl bis(6-butyldodecanoate) (CL4F 12_ε-4)

Synthesis of 2-butyloctanal

2-Butyl-1-n-octanol (1.86 g, 10 mmol) was dissolved in anhydrous DCM (30 mL) and TEMPO (15.5 mg, 0.10 mmol), Bu_4NHSO_4 (0.17 g, 0.50 mmol) was added and the mixture was cooled on ice. NaOCl-$5H_2O$ (1.98 g, 12.0 mmol) was added, and the reaction mixture was stirred on ice for 3 h. The reaction mixture was quenched with sat. $Na_2S_2O_3$ aq. and diluted with EtOAc and was washed with water and brine and dried over anhydrous Na_2SO_4. The solution was filtered, and the filtrate was evaporated. The residue was loaded onto a normal-phase column (Sfär Silica HC D, Biotage), and purified by flash chromatography (Selekt, Biotage) with a gradient mobile phase of hexane and EtOAc. This gave 1.86 g (101%) of 2-butyloctanal as a colorless oil.

Synthesis of ethyl 6-hexyldodec-4-enoate

To a stirred suspension of (4-ethoxy-4-oxobutyl) triphenyl phosphonium bromide (5.49 g, 12.0 mmol) in anhydrous THF (12 mL) under an Ar atmosphere cooled to 0°C was added potassium *tert*-butoxide (1 M solution in THF) (12.0 mL) dropwise. The reaction mixture was stirred at room temperature for 30 min, then 2-butyloctanal (1.86 g, 10.0 mmol) was added, and the reaction mixture was stirred at room temperature overnight. The reaction mixture was quenched with sat. NH_4Cl aq. and diluted with Et_2O, washed with brine, and dried over anhydrous

Na_2SO_4. The solution was filtered, and the filtrate was evaporated. The residue was dissolved in hexane and through silica gel, and the solution was evaporated. The residue was loaded onto a normal-phase column (Sfär Silica HC D, Biotage), and purified by flash chromatography (Selekt, Biotage) with a gradient mobile phase of hexane and EtOAc. This gave 1.75 g of ethyl 6-butyldodec-4-enoate as a colorless oil.

Synthesis of ethyl 6-butyldodecanoate

Ethyl 6-butyldodec-4-enoate (1.75 g) was dissolved in a mixture of MeOH (10 mL) and DCM (10 mL) under an Ar atmosphere. Pd/C (175 mg, 10 wt %) was added. The mixture was hydrogenated under balloon pressure at ambient temperature overnight. The reaction mixture was filtered through a small pad of celite, and washed with DCM. The filtrate was evaporated. This gave 1.75 g of ethyl 6-butyldodecanoate as a cloudy white oil. The crude product was used for the next reaction without further purification.

Synthesis of 6-butyldodecanoic acid

Ethyl 6-butyldodecanoate (1.75 g) was dissolved in a mixture of 2-propanol (4.0 mL) and water (2.0 mL). KOH (0.67 g, 12 mmol) was added, and the reaction mixture was stirred at 70°C overnight. The reaction mixture was cooled to room temperature, hexane was added and the mixture was washed with 1 N HCl aq., water, brine, and was dried over anhydrous Na_2SO_4. The solution was filtered, and the filtrate was evaporated. This gave 1.59 g of 6-butyldodecanoic acid as a yellow oil. The crude product was used for the next reaction without further purification.

Synthesis of 7-(4-(dipropylamino)butyl)-7-hydroxytridecane-1,13-diyl bis(6-butyldodecanoate)

6-Butyldodecanoic acid (1.59 g) was dissolved in anhydrous DCM (10 mL) and 7-(4-dipropylamino)butyl)tridecane-1,7,13-triol (210 mg, 0.55 mmol); DMAP (6.7 mg, 0.055 mmol) and EDCI-HCl (260 mg, 1.38 mmol) were added to the mixture. The reaction mixture was stirred at ambient temperature overnight. The reaction mixture was evaporated. The residue was suspended with EtOAc, washed with 0.5 N NaOH aq. and brine, and dried over anhydrous Na_2SO_4. The solution was filtered, and the filtrate was evaporated. The residue was loaded onto a reverse-phase column (HP C18Aq, Teledyne ISCO), and purified by flash chromatography (CombiFlash Rf, Teledyne ISCO) with a gradient mobile phase of water with 0.1% TFA and acetonitrile/2-propanol (1:1) with 0.1% TFA. This residue was loaded onto a normal-phase column (Sfär Silica HC D, Biotage), and was purified by flash chromatography (Slekt, Biotage) with a gradient mobile phase of DCM and MeOH. This gave 85 mg (18%) of 7-(4-(dipropylamino)butyl)-7-hydroxytridecane-1,13-diyl bis(6-butyldodecanoate) (CL4F 12_ε-4) as a colorless oil.

Synthesis of 7-(4-(dipropylamino)butyl)-7-hydroxytridecane-1,13-diyl bis(6-hexyldodecanoate) (CL4F 12_ε-6)

Synthesis of 2-hexyloctanal

2-Hexyl-1-n-octanol (2.14 g, 10 mmol) was dissolved in anhydrous DCM (30 mL); TEMPO (15.5 mg, 0.10 mmol) and Bu_4NHSO_4 (0.17 g, 0.50 mmol) were added, and the mixture was cooled on ice. NaOCl-$5H_2O$ (1.98 g, 12.0 mmol) was added, and the reaction mixture was stirred on ice for 3 h. The reaction mixture was quenched with sat. $Na_2S_2O_3$ aq. and diluted with EtOAc and was washed with water and brine and dried over anhydrous Na_2SO_4. The solution was filtered, and the filtrate was evaporated. The residue was loaded onto a normal-phase column (Sfär Silica HC D, Biotage), and purified by flash chromatography (Selekt, Biotage) with a gradient mobile phase of hexane and EtOAc. This gave 1.81 g (85%) of 2-hexyloctanal as a colorless oil.

Synthesis of ethyl 6-hexyldodec-4-enoate

To a stirred suspension of (4-ethoxy-4-oxobutyl) triphenyl phosphonium bromide (4.67 g, 10.2 mmol) in anhydrous THF (8 mL) under an Ar atmosphere cooled to −78°C was added potassium *tert*-butoxide (1 M solution in THF) (10.2 mL) dropwise. The reaction mixture was stirred at −78°C for 30 min, and then 2-hexyloctanal (1.81 g) was added. The reaction mixture was gradually warmed to room temperature overnight. The reaction mixture was quenched with sat. NH_4Cl aq. and diluted with Et_2O and was washed with brine and dried over anhydrous Na_2SO_4. The solution was filtered, and the filtrate was evaporated. The residue was dissolved in hexane and through silica gel, and the solution was evaporated. The residue was loaded onto a normal-phase column (Sfär Silica HC D, Biotage), and purified by flash chromatography (Selekt, Biotage) with a gradient mobile phase of hexane and EtOAc. This gave 1.93 g (73%) of ethyl 6-hexyldodec-4-enoate as a colorless oil.

Synthesis of ethyl 6-hexyldodecanoate

Ethyl 6-hexyldodec-4-enoate (1.93 g, 6.2 mmol) was dissolved in a mixture of MeOH (10 mL) and DCM (10 mL) under an Ar atmosphere. Pd/C (193 mg, 10 wt %) was added. The mixture was hydrogenated under balloon pressure at ambient temperature overnight. The reaction mixture was filtered through a small pad of celite, and washed with DCM. The filtrate was evaporated. This gave 1.95 g (101%) of ethyl 6-hexyldodecanoate as a cloudy white oil. The crude product was used for the next reaction without further purification.

Synthesis of 6-hexyldodecanoic acid

Ethyl 6-hexyldodecanoate (1.95 g, 6.2 mmol) was dissolved in a mixture of 2-propanol (21 mL) and water (10.5 mL). KOH (3.48 g, 62 mmol) was added, and the reaction mixture was stirred at 70°C overnight. The reaction mixture was cooled to room temperature, hexane was added, and then was washed with 1 N HCl aq., water, and brine, and dried over anhydrous Na_2SO_4. The solution was filtered, and the filtrate was

evaporated. This gave 1.73 g (98%) of 6-hexyldodecanoic acid as a yellow oil. The crude product was used for the next reaction without further purification.

Synthesis of 7-(4-(dipropylamino)butyl)-7-hydroxytridecane-1,13-diyl bis(3-octylundecanoate)

6-Hexyldodecanoic acid (1.2 g, 4.2 mmol) was dissolved in anhydrous DCM (10 mL) and 7-(4-dipropylamino)butyl)tridecane-1,7,13-triol (757 mg, 1.95 mmol); DMAP (24.4 mg, 0.2 mmol) and EDCI-HCl (930 mg, 4.9 mmol) were added to the mixture. The reaction mixture was stirred at ambient temperature overnight. The reaction mixture was evaporated. The residue was suspended with EtOAc, washed with 0.5 N NaOH aq. and brine, and dried over anhydrous Na_2SO_4. The solution was filtered, and the filtrate was evaporated. The residue was loaded onto a reverse-phase column (HP C18Aq, Teledyne ISCO), and purified by flash chromatography (CombiFlash Rf, Teledyne ISCO) with a gradient mobile phase of water with 0.1% TFA and acetonitrile/2-propanol (1:1) with 0.1% TFA. This residue was loaded onto a normal-phase column (Sfär Silica HC D, Biotage), and purified by flash chromatography (Slekt, Biotage) with a gradient mobile phase of DCM and MeOH. This gave 320 mg (18%) of 7-(4-(dipropylamino)butyl)-7-hydroxytridecane-1,13-diyl bis(6-hexyldodecanoate) (CL4F 12_ε-6) as a yellow oil.

Synthesis of 7-(4-(dipropylamino)butyl)-7-hydroxytridecane-1,13-diyl bis(7-ethylundecanoate) (CL4F 11_ζ-2)

Synthesis of 7-ethylundec-5-enoic acid

To a stirred suspension of 4-(carboxybutyl) triphenyl phosphonium bromide (2.66 g, 6.0 mmol) in anhydrous THF (6 mL) under an Ar atmosphere cooled to −78°C was added potassium *tert*-butoxide (1 M solution in THF) (12 mL) dropwise. The reaction mixture was stirred at −78°C for 30 min, then 2-ethylhexanal (0.64 g, 5.0 mmol) was added. The reaction mixture was gradually warmed to room temperature overnight. The reaction mixture was quenched with sat. NH_4Cl aq. and diluted with Et_2O and was washed with brine and dried over anhydrous Na_2SO_4. The solution was filtered, and the filtrate was evaporated. This gave 0.69 g (65%) of ethylundec-5-enoic acid as a colorless oil. The crude product was used for the next reaction without further purification.

Synthesis of 7-ethylundecanoic acid

Ethylundec-5-enoic acid (0.69 g, 3.2 mmol) was dissolved in a mixture of MeOH (10 mL) and DCM (10 mL) under an Ar atmosphere. Pd/C (69 mg, 10 wt %) was added. The mixture was hydrogenated under balloon pressure at ambient temperature overnight. The reaction mixture was filtered through a small pad of celite, and washed with DCM. The filtrate was evaporated. This gave 0.69 g (100%) of 7-ethylundecanoic acid as a cloudy white oil. The crude product was used for the next reaction without further purification.

Synthesis of 7-(4-(dipropylamino)butyl)-7-hydroxytridecane-1,13-diyl bis(7-ethylundecanoate)

7-Ethylundecanoic acid (0.69 g, 3.2 mmol) was dissolved in anhydrous DCM (10 mL) and 7-(4-dipropylamino)butyl)tridecane-1,7,13-triol (562 mg, 1.45 mmol); DMAP (18 mg, 0.15 mmol) and EDCI-HCl (690 mg, 3.6 mmol) were added to the mixture. The reaction mixture was stirred at ambient temperature overnight. The reaction mixture was evaporated. The residue was suspended with EtOAc, washed with 0.5 N NaOH aq. and brine, and dried over anhydrous Na_2SO_4. The solution was filtered, and the filtrate was evaporated. The residue was loaded onto a reverse-phase column (Sfär C18, Biotage), and purified by flash chromatography (Slekt, Biotage) with a gradient mobile phase of water with 0.1% TFA and acetonitrile/2-propanol (1:1) with 0.1% TFA. This residue was loaded onto a normal-phase column (Sfär Silica HC D, Biotage), and purified by flash chromatography (Slekt, Biotage) with a gradient mobile phase of DCM and MeOH. This gave 472 mg (42%) of 7-(4-(dipropylamino)butyl)-7-hydroxytridecane-1,13-diyl bis(7-ethylundecanoate) (CL4F 11_ζ-2) as an colorless oil.

Synthesis of 7-(4-(dipropylamino)butyl)-7-hydroxytridecane-1,13-diyl bis(8-ethyldodecanoate) (CL4F 12_η-2)

Synthesis of 8-ethyldodec-6-enoic acid

To a stirred suspension of 5-(carboxypentyl) triphenyl phosphonium bromide (2.74 g, 6.0 mmol) in anhydrous THF (6 mL) under an Ar atmosphere cooled to −78°C was added potassium *tert*-butoxide (1 M solution in THF) (12 mL) dropwise. The reaction mixture was stirred at −78°C for 30 min, then 2-ethylhexanal (0.64 g, 5.0 mmol) was added. The reaction mixture was gradually warmed to room temperature overnight. The reaction mixture was quenched with sat. NH_4Cl aq. and diluted with Et_2O and was washed with brine and dried over with anhydrous Na_2SO_4. The solution was filtered, and the filtrate was evaporated. This gave 0.85 g (75%) of 8-ethyldodec-6-enoic acid as a colorless oil. The crude product was used for the next reaction without further purification.

Synthesis of 8-ethyldodecanoic acid

8-Ethyldodec-6-enoic acid (0.85 g, 3.7 mmol) was dissolved in a mixture of MeOH (10 mL) and DCM (10 mL) under an Ar atmosphere. Pd/C (85 mg, 10 wt %) was added. The mixture was hydrogenated under balloon pressure at ambient temperature overnight. The reaction mixture was filtered through a small pad of celite, and washed with DCM. The filtrate was evaporated. This gave 0.86 g (102%) of 8-ethyldodecanoic acid as a cloudy white oil. The crude product was used for the next reaction without further purification.

Synthesis of 7-(4-(dipropylamino)butyl)-7-hydroxytridecane-1,13-diyl bis(8-ethyldodecanoate)

8-Ethyldodecanoic acid (0.55 g, 2.4 mmol) was dissolved in anhydrous DCM (10 mL) and 7-(4-dipropylamino)butyl)tridecane-1,7,13-triol (430 mg, 1.1 mmol); DMAP (13 mg, 0.11 mmol) and EDCI-HCl (527 mg, 2.75 mmol) were added to the mixture. The reaction mixture was evaporated after being stirred at ambient temperature overnight. The residue was suspended with EtOAc, washed with 0.5 N NaOH aq. and brine, and dried over anhydrous Na_2SO_4. The solution was filtered, and the filtrate was evaporated. The residue was loaded onto a reverse-phase column (Sfär C18, Biotage), and purified by flash chromatography (Slekt, Biotage) with a gradient mobile phase of water with 0.1% TFA and acetonitrile/2-propanol (1:1) with 0.1% TFA. This residue was loaded onto a normal-phase column (Sfär Silica HC D, Biotage), and purified by flash chromatography (Slekt, Biotage) with a gradient mobile phase of DCM and MeOH. This gave 202 mg (23%) of 7-(4-(dipropylamino)butyl)-7-hydroxytridecane-1,13-diyl bis(8-ethyldodecanoate) (CL4F 12_η-2) as a yellow oil.

Synthesis of 7-(4-(dipropylamino)butyl)-7-hydroxytridecane-1,13-diyl bis(8,10,10-trimethylundecanoate) (CL4F 11_η-3(3))

Synthesis of 3,5,5-trimethylhexanal

3,5,5-Trimethylhexana-1-ol (1.44 g, 10 mmol) was dissolved in anhydrous DCM (30 mL); TEMPO (15.5 mg, 0.10 mmol) and Bu_4NHSO_4 (0.17 g, 0.50 mmol) were added, and the mixture was cooled on ice. NaOCl-$5H_2O$ (1.98 g, 12.0 mmol) was added, and the reaction mixture was stirred on ice for 3 h. The reaction mixture was quenched with sat. $Na_2S_2O_3$ aq. and diluted with EtOAc and was washed with water and brine and dried over anhydrous Na_2SO_4. The solution was filtered, and the filtrate was evaporated. This gave 0.91 g (64%) of 3,5,5-trimethylhexanal as a yellow oil. The crude product was used for the next reaction without further purification.

Synthesis of 8,10,10-trimethylundec-5-enoic acid

To a stirred suspension of 5-(carboxybutyl) triphenyl phosphonium bromide (2.74 g, 6.0 mmol) in anhydrous THF (6 mL) under an Ar atmosphere cooled to −78°C was added potassium *tert*-butoxide (1 M solution in THF) (12 mL) dropwise. The reaction mixture was stirred at −78°C for 30 min, then 3,5,5-trimethylhexanal (0.91 g) was added. The reaction mixture was gradually warmed to room temperature overnight. The reaction mixture was quenched with sat. NH_4Cl aq., diluted with Et_2O, washed with brine, and dried over anhydrous Na_2SO_4. The solution was filtered, and the filtrate was evaporated. The residue was loaded onto a reverse-phase column (Sfär C18, Biotage), and purified by flash chromatography (Slekt, Biotage) with a gradient mobile phase of water with 0.1% TFA and acetonitrile with 0.1% TFA. This gave 0.42 g (37%) of 8,10,10-trimethylundec-5-enoic acid as a colorless oil.

Synthesis of 8,10,10-trimethylundecanoic acid

8,10,10-Trimethylundec-5-enoic acid (0.42 g, 1.9 mmol) was dissolved in a mixture of MeOH (10 mL) and DCM (10 mL) under an Ar atmosphere. Pd/C (42 mg, 10 wt %) was added. The mixture was hydrogenated under balloon pressure at ambient temperature overnight. The reaction mixture was filtered through a small pad of celite, and washed with DCM. The filtrate was evaporated. This gave 0.42 g (99%) of 8,10,10-trimethylundecanoic acid as a cloudy white oil. The crude product was used for the next reaction without further purification.

Synthesis of 7-(4-(dipropylamino)butyl)-7-hydroxytridecane-1,13-diyl bis(8,10,10-trimethylundecanoate)

8,10,10-Trimethylundecanoic acid (0.42 g, 1.8 mmol) was dissolved in anhydrous DCM (10 mL) and 7-(4-dipropylamino)butyl)tridecane-1,7,13-triol (318 mg, 0.8 mmol); DMAP (10 mg, 0.1 mmol) and EDCI-HCl (383 mg, 2.0 mmol) were added to the mixture. The reaction mixture was evaporated after being stirred at ambient temperature overnight. The residue was suspended with EtOAc, washed with 0.5 N NaOH aq. and brine, and dried over anhydrous Na_2SO_4. The solution was filtered, and the filtrate was evaporated. The residue was loaded onto a reverse-phase column (Sfär C18, Biotage), and purified by flash chromatography (Slekt, Biotage) with a gradient mobile phase of water with 0.1% TFA and acetonitrile/2-propanol (1:1) with 0.1% TFA. This residue was loaded onto a normal-phase column (Sfär Silica HC D, Biotage), and purified by flash chromatography (Slekt, Biotage) with a gradient mobile phase of DCM and MeOH. This gave 251 mg (38%) of 7-(4-(dipropylamino) butyl)-7-hydroxytridecane-1,13-diyl bis(8,10,10-trimethylundecanoate) (CL4F 11_η-3(3)) as a colorless oil.

Synthesis of 7-(4-(dipropylamino)butyl)-7-hydroxytridecane-1,13-diyl bis(7,9,9-trimethyldecanoate) (CL4F 10_ζ-3(3))

Synthesis of 3,5,5-trimethylhexanal

3,5,5-Trimethylhexana-1-ol (1.44 g, 10.0 mmol) was dissolved in anhydrous DCM (30 mL); TEMPO (15.5 mg, 0.10 mmol) and Bu_4NHSO_4 (0.17 g, 0.50 mmol) were added, and the mixture was cooled on ice. NaOCl-$5H_2O$ (1.98 g, 12.0 mmol) was added, and the reaction mixture was stirred on ice for 3 h. The reaction mixture was quenched with sat. $Na_2S_2O_3$ aq., diluted with EtOAc, washed with water and brine, and dried over anhydrous Na_2SO_4. The solution was filtered, and the filtrate was evaporated. This gave 1.18 g (83%) of 3,5,5-trimethylhexanal as a yellow oil. The crude product was used for the next reaction without further purification.

Synthesis of 7,9,9-trimethyldec-4-enoic acid

To a stirred suspension of 3-(carboxypropyl) triphenyl phosphonium bromide (4.3 g, 10.0 mmol) in anhydrous THF (6 mL) under an Ar atmosphere cooled to −78°C was added potassium *tert*-butoxide (1 M solution in THF) (20 mL) dropwise. The reaction mixture was stirred at −78°C for 30 min, then 3,5,5-trimethylhexanal (1.18 g) was added. The reaction mixture was gradually warmed to room temperature overnight. The

reaction mixture was quenched with sat. NH_4Cl aq., diluted with Et_2O, washed with brine, and dried over anhydrous Na_2SO_4. The solution was filtered, and the filtrate was evaporated. The residue was loaded onto a reverse-phase column (Sfär C18, Biotage), and purified by flash chromatography (Slekt, Biotage) with a gradient mobile phase of water with 0.1% TFA and acetonitrile with 0.1% TFA. This gave 0.51 g (29%) of 7,9,9-trimethyldec-4-enoic acid as a yellow oil.

Synthesis of 7,9,9-trimethyldecanoic acid

7,9,9-Trimethyldec-4-enoic acid (0.51 g, 2.4 mmol) was dissolved in a mixture of MeOH (10 mL) and DCM (10 mL) under an Ar atmosphere. Pd/C (51 mg, 10 wt %) was added. The mixture was hydrogenated under balloon pressure at ambient temperature overnight. The reaction mixture was filtered through a small pad of celite, and washed with DCM. The filtrate was evaporated. This gave 0.51 g (99%) of 7,9,9-trimethyldecanoic acid as a cloudy white oil. The crude product was used for the next reaction without further purification.

Synthesis of 7-(4-(dipropylamino)butyl)-7-hydroxytridecane-1,13-diyl bis(7,9,9-trimethyldecanoate)

7,9,9-Trimethyldecanoic acid (0.51 g, 2.4 mmol) was dissolved in anhydrous DCM (10 mL) and 7-(4-dipropylamino)butyl)tridecane-1,7,13-triol (426 mg, 1.1 mmol); DMAP (13 mg, 0.1 mmol) and EDCI-HCl (518 mg, 2.7 mmol) were added to the mixture. The reaction mixture was evaporated after being stirred at ambient temperature overnight. The residue was suspended with EtOAc, washed with 0.5 N NaOH aq. and brine, and dried over anhydrous Na_2SO_4. The solution was filtered, and the filtrate was evaporated. The residue was loaded onto a reverse-phase column (Sfär C18, Biotage), and purified by flash chromatography (Slekt, Biotage) with a gradient mobile phase of water with 0.1% TFA and acetonitrile/2-propanol (1:1) with 0.1% TFA. This residue was loaded onto a normal-phase column (Sfär Silica HC D, Biotage), and purified by flash chromatography (Slekt, Biotage) with a gradient mobile phase of DCM and MeOH. This gave 75 mg (9%) of 7-(4-(dipropylamino)butyl)-7-hydroxytridecane-1,13-diyl bis(7,9,9-trimethyldecanoate) (CL4F 10_ζ-3(3)) as a yellow oil.

Synthesis of 7-(4-(dipropylamino)butyl)-7-hydroxytridecane-1,13-diyl bis(9,11,11-trimethyldodecanoate) (CL4F 12_θ-3(3))

Synthesis of 3,5,5-trimethylhexanal

3,5,5-Trimethylhexana-1-ol (1.44 g, 10.0 mmol) was dissolved in anhydrous DCM (30 mL); TEMPO (15.5 mg, 0.10 mmol) and Bu_4NHSO_4 (0.17 g, 0.50 mmol) were added, and the mixture was cooled on ice. NaOCl-$5H_2O$ (1.98 g, 12.0 mmol) was added, and the reaction mixture was stirred on ice for 3 h. The reaction mixture was quenched with sat. $Na_2S_2O_3$ aq., diluted with EtOAc, washed with water and brine, and dried over anhydrous Na_2SO_4. The solution was filtered, and the filtrate was evaporated. This gave 1.37 g (94%) of 3,5,5-trimethylhexanal as a yellow oil. The crude product was used for the next reaction without further purification.

Synthesis of 9,11,11-trimethyldodec-6-enoic acid

To a stirred suspension of 5-(carboxypentyl) triphenyl phosphonium bromide (5.2 g, 11.3 mmol) in anhydrous THF (6 mL) under an Ar atmosphere cooled to −78°C was added potassium *tert*-butoxide (1 M solution in THF) (23 mL) dropwise. The reaction mixture was stirred at −78°C for 30 min, then 3,5,5-trimethylhexanal (1.37 g) was added. The reaction mixture was gradually warmed to room temperature overnight. The reaction mixture was quenched with sat. NH_4Cl aq., diluted with Et_2O, washed with brine, and dried over anhydrous Na_2SO_4. The solution was filtered, and the filtrate was evaporated. The residue was loaded onto a reverse-phase column (Sfär C18, Biotage), and purified by flash chromatography (Slekt, Biotage) with a gradient mobile phase of water with 0.1% TFA and acetonitrile with 0.1% TFA. This gave 0.47 g (21%) of 9,11,11-trimethyldodec-6-enoic acid as a colorless oil.

Synthesis of 9,11,11-trimethyldodecanoic acid

9,11,11-Trimethyldodec-6-enoic acid (0.47 g, 2.0 mmol) was dissolved in a mixture of MeOH (10 mL) and DCM (10 mL) under an Ar atmosphere. Pd/C (47 mg, 10 wt %) was added. The mixture was hydrogenated under balloon pressure at ambient temperature overnight. The reaction mixture was filtered through a small pad of celite, and washed with DCM. The filtrate was evaporated. This gave 0.47 g (96%) of 9,11,11-trimethyldodecanoic acid as a cloudy white oil. The crude product was used for the next reaction without further purification.

Synthesis of 7-(4-(dipropylamino)butyl)-7-hydroxytridecane-1,13-diyl bis(9,11,11-trimethyldodecanoate)

9,11,11-Trimethyldodecanoic acid (0.47 g, 1.9 mmol) was dissolved in anhydrous DCM (10 mL) and 7-(4-dipropylamino)butyl)tridecane-1,7,13-triol (333 mg, 0.9 mmol); DMAP (11 mg, 0.1 mmol) and EDCI-HCl (414 mg, 2.2 mmol) were added to the mixture. The reaction mixture was stirred at ambient temperature overnight. The reaction mixture was evaporated. The residue was suspended with EtOAc, washed with 0.5 N NaOH aq. and brine, and dried over anhydrous Na_2SO_4. The solution was filtered, and the filtrate was evaporated. The residue was loaded onto a reverse-phase column (Sfär C18, Biotage), and purified by flash chromatography (Slekt, Biotage) with a gradient mobile phase of water with 0.1% TFA and acetonitrile/2-propanol (1:1) with 0.1% TFA. This residue was loaded onto a normal-phase column (Sfär Silica HC D, Biotage), and purified by flash chromatography (Slekt, Biotage) with a gradient mobile phase of DCM and MeOH. This gave 233 mg (32%) of 7-(4-(dipropylamino)butyl)-7-hydroxytridecane-1,13-diyl bis(9,11,11-trimethyldodecanoate) (CL4F 12_θ-3(3)) as a yellow oil.

Synthesis of 7-(4-(dipropylamino)butyl)-7-hydroxytridecane-1,13-diyl bis(7,11-dimethyldodecanoate) (CL4F 12_ζ-2(2))

Synthesis of 3,7-dimethyloctanal

3,7-dimethyloctan-1-ol (1.58 g, 10.0 mmol) was dissolved in anhydrous DCM (30 mL); TEMPO (15.5 mg, 0.10 mmol) and Bu_4NHSO_4 (0.17 g, 0.50 mmol) were added, and the mixture was cooled on ice. NaOCl-$5H_2O$ (1.98 g, 12.0 mmol) was added, and the reaction mixture was stirred on ice for 3 h. The reaction mixture was quenched with sat. $Na_2S_2O_3$ aq., diluted with EtOAc, washed with water and brine, and dried over anhydrous Na_2SO_4. The solution was filtered, and the filtrate was evaporated. This gave 1.59 g (102%) of 3,7-dimethyloctanal as a colorless oil. The crude product was used for the next reaction without further purification.

Synthesis of 7,11-dimethyldodec-4-enoic acid

To a stirred suspension of 3-(carboxypropyl) triphenyl phosphonium bromide (5.2 g, 12.0 mmol) in anhydrous THF (6 mL) under an Ar atmosphere cooled to −78°C was added potassium *tert*-butoxide (1 M solution in THF) (24 mL) dropwise. The reaction mixture was stirred at −78°C for 30 min, then 3,7-dimethyloctanal (1.59 g) was added. The reaction mixture was gradually warmed to room temperature overnight. The reaction mixture was quenched with sat. NH_4Cl aq., diluted with Et_2O, washed with brine, and dried over anhydrous Na_2SO_4. The solution was filtered, and the filtrate was evaporated. The residue was loaded onto a reverse-phase column (Sfär C18, Biotage), and purified by flash chromatography (Slekt, Biotage) with a gradient mobile phase of water with 0.1% TFA and acetonitrile with 0.1% TFA. This gave 0.90 g (40%) of 7,11-dimethyldodec-4-enoic acid as a colorless oil.

Synthesis of 7,11-dimethyldodecanoic acid

7,11-dimethyldodec-4-enoic acid (0.90 g, 4.0 mmol) was dissolved in a mixture of MeOH (10 mL) and DCM (10 mL) under an Ar atmosphere. Pd/C (90 mg, 10 wt %) was added. The mixture was hydrogenated under balloon pressure at ambient temperature overnight. The reaction mixture was filtered through a small pad of celite, and washed with DCM. The filtrate was evaporated. This gave 0.90 g (99%) of 7,11-dimethyldodecanoic acid as a cloudy white oil. The crude product was used for the next reaction without further purification.

Synthesis of 7-(4-(dipropylamino)butyl)-7-hydroxytridecane-1,13-diyl bis(9,11,11-trimethyldodecanoate)

9,11,11-Trimethyldodecanoic acid (0.90 g, 4.0 mmol) was dissolved in anhydrous DCM (10 mL) and 7-(4-dipropylamino)butyl)tridecane-1,7,13-triol (698 mg, 1.8 mmol); DMAP (22 mg, 0.2 mmol) and EDCI-HCl (861 mg, 4.5 mmol) were added to the mixture. The reaction mixture was stirred at ambient temperature overnight. The reaction mixture was evaporated. The residue was suspended with EtOAc, washed with 0.5 N NaOH aq. and brine, and dried over anhydrous Na_2SO_4. The solution was filtered, and the filtrate was evaporated. The residue was loaded onto a reverse-phase column (Sfär C18, Biotage), and purified by flash chromatography (Slekt, Biotage) with a gradient mobile phase of water with 0.1% TFA and acetonitrile/2-propanol (1:1) with 0.1% TFA. This residue was loaded onto a normal-phase column (Sfär Silica HC D, Biotage), and purified by flash chromatography (Slekt, Biotage) with a gradient mobile phase of DCM and MeOH. This gave 306 mg (21%) of 7-(4-(dipropylamino)butyl)-7-hydroxytridecane-1,13-diyl bis(7,11-dimethyldodecanoate) (CL4F 12_ζ-2(2)) as a yellow oil.

Synthesis of 7-(4-(dipropylamino)butyl)-7-hydroxytridecane-1,13-diyl bis(8,12-dimethyltridecanoate) (CL4F 13_η-2(2))

Synthesis of 3,7-dimethyloctanal

3,7-dimethyloctan-1-ol (1.58 g, 10.0 mmol) was dissolved in anhydrous DCM (30 mL); TEMPO (15.5 mg, 0.10 mmol) and Bu_4NHSO_4 (0.17 g, 0.50 mmol) were added, and the mixture was cooled on ice. NaOCl-$5H_2O$ (1.98 g, 12.0 mmol) was added, and the reaction mixture was stirred on ice for 3 h. The reaction mixture was quenched with sat. $Na_2S_2O_3$ aq., diluted with EtOAc, washed with water and brine, and dried over anhydrous Na_2SO_4. The solution was filtered, and the filtrate was evaporated. This gave 1.63 g (104%) of 3,7-dimethyloctanal as a colorless oil. The crude product was used for the next reaction without further purification.

Synthesis of 8,12-dimethyltridecanoic acid

To a stirred suspension of 4-(carboxybutyl) triphenyl phosphonium bromide (5.3 g, 12.0 mmol) in anhydrous THF (6 mL) under an Ar atmosphere cooled to −78°C was added potassium *tert*-butoxide (1 M solution in THF) (24 mL) dropwise. The reaction mixture was stirred at −78°C for 30 min, then 3,7-dimethyloctanal (1.63 g) was added. The reaction mixture was gradually warmed to room temperature overnight. The reaction mixture was quenched with sat. NH_4Cl aq., diluted with Et_2O, washed with brine, and dried over anhydrous Na_2SO_4. The solution was filtered, and the filtrate was evaporated. The residue was loaded onto a reverse-phase column (Sfär C18, Biotage), and purified by flash chromatography (Slekt, Biotage) with a gradient mobile phase of water with 0.1% TFA and acetonitrile with 0.1% TFA. This gave 0.77 g (32%) of 8,12-dimethyltridecanoic acid as a colorless oil.

Synthesis of 8,12-dimehtyltridecanoic acid

8,12-dimethyltridecanoic acid (0.90 g, 4.0 mmol) was dissolved in a mixture of MeOH (10 mL) and DCM (10 mL) under an Ar atmosphere. Pd/C (90 mg, 10 wt %) was added. The mixture was hydrogenated under balloon pressure at ambient temperature overnight. The reaction mixture was filtered through a small pad of celite, and washed with DCM. The filtrate was evaporated. This gave 0.76 g (98%) of 8,12-dimethyltridecanoic acid as a cloudy white oil. The crude product was used for the next reaction without further purification.

Synthesis of 7-(4-(dipropylamino)butyl)-7-hydroxytridecane-1,13-diyl bis(8,12-dimethyltridecanoate)

8,12-dimethyltridecanoic acid (0.76 g, 3.1 mmol) was dissolved in anhydrous DCM (10 mL) and 7-(4-dipropylamino)butyl)tridecane-1,7,13-triol (553 mg, 1.4 mmol); DMAP (17 mg, 0.1 mmol) and EDCI-HCl (684 mg, 3.6 mmol) were added to the mixture. The reaction mixture was evaporated after being stirred at ambient temperature overnight. The residue was suspended with EtOAc, washed with 0.5 N NaOH aq. and brine, and dried over anhydrous Na_2SO_4. The solution was filtered, and the filtrate was evaporated. The residue was loaded onto a reverse-phase column (Sfär C18, Biotage), and purified by flash chromatography (Slekt, Biotage) with a gradient mobile phase of water with 0.1% TFA and acetonitrile/2-propanol (1:1) with 0.1% TFA. This residue was loaded onto a normal-phase column (Sfär Silica HC D, Biotage), and purified by flash chromatography (Slekt, Biotage) with a gradient mobile phase of DCM and MeOH. This gave 558 mg (47%) of 7-(4-(dipropylamino)butyl)-7-hydroxytridecane-1,13-diyl bis(8,12-dimethyltridecanoate) (CL4F 13_η-2(2)) as a yellow oil.

Preparation of RNP-loaded LNPs

RNP-loaded LNPs were prepared as previously reported.[18,19] A solution of Cas protein (10 μM) was titrated to an equal volume of sgRNA solution (10 μM) under vigorous mixing to produce 5 μM of an RNP solution. The RNP solution was mixed with an equal volume of an ssODN solution (5 μM) to obtain 2.5 μM of RNP-ssODN complexes. The ssODN is designed to contain a sequence complementary to the target sequence of the corresponding sgRNA with a Tm around 24°C. This allows ssODNs to complex with RNPs, increasing the negative charge of RNPs and enhancing their electrostatic interaction with ionizable lipids, thereby promoting RNP encapsulation.[19] An ethanol solution containing ionizable lipid, DSPC, chol, and PEG-DMG in a molar ratio of 50/10/40/3.5 was prepared to achieve a total lipid concentration of 8 mM. The total of the three lipid components, excluding PEG-DMG, is expressed as 100 mol %. For the fluorescent labeling of the LNPs, either 0.005 mol % of DiD (for *in vitro* cellular uptake study) or 0.1–0.5 mol % of DiR (for *in vivo* biodistribution study) was added to the above solution. The RNP-ssODN was diluted to 160 nM in 20 mM MES buffer (pH 6.0, 50 mM NaCl). RNP-loaded LNPs were prepared by mixing the lipids in ethanol and RNP-ssODN in an aqueous solution using a polydimethylsiloxane-based iLiNP device (1 mm width) at a total flow rate of 2.0 mL/min (0.20 mL/min for the lipid solution and 1.80 mL/min for the RNP-ssODN solution). Syringe pumps (Harvard apparatus, MA, USA) were used to control the flow rate. The resultant LNP solution was dialyzed for 2 h or more at 4°C against PBS(−) using Spectra/Por 4 dialysis membranes (molecular weight cut-off 12–14 kDa, Spectrum Laboratories, CA, USA) and was then concentrated via ultrafiltration using an Amicon Ultra-15 (MWCO 100 kDa, Millipore). In order to evaluate tolerability against a freeze/thaw cycle, the LNP solution was dialyzed against 20 mM tris-HCl buffer (pH7.4) containing 9% sucrose as a cryoprotectant.

Preparation of RNA-loaded LNPs

RNA-loaded LNPs were prepared as previously reported.[52] Ethanol solutions containing ionizable lipid, DSPC, chol, and PEG-DMG in ratios of either 50/10/40/1.0 (for siRNA) or 50/10/40/1.5 (for mRNA) were prepared to achieve total lipid concentrations of 8 mM. For the fluorescent labeling of the LNPs, 0.005 mol % of DiD (for *in vitro* cellular uptake study) or 0.1–0.5 mol % of DiR (for *in vivo* biodistribution study) was added to the above solution. The RNA was dissolved in 25 mM of acetate buffer (pH 4.0). The nitrogen/phosphate ratio was fixed at 9. LNPs were prepared by mixing the lipids in ethanol and RNA in an aqueous solution using an iLiNP device at a combined flow rate of 0.5 mL/min (0.125 mL/min for the lipid solution and 0.375 mL for the RNA solution). Syringe pumps were used to control the flow rate. The resultant LNP solution was then dialyzed for 2 h or more at 4°C against PBS(−) using Spectra/Por 4 dialysis membranes. The LNP solution was concentrated by ultrafiltration using an Amicon Ultra-15 unit (MWCO 100 kDa) as needed.

Characterization of the LNPs

The size (ζ-average), polydispersity index (PdI), and ζ-potential of the LNPs were measured by means of a Zetasizer Nano ZS ZEN3600 instrument (Malvern Instruments, Worchestershire, UK). The LNPs were diluted using D-PBS(−) and 10 mM of HEPES buffer at pH 7.4 for size and ζ-potential measurements, respectively. The apparent pKa value of the LNPs was measured by TNS assay as described previously.[53] The encapsulation efficiency (% encapsulation) and total concentration of RNP-ssODN and RNA, respectively, were measured via Ribogreen assay as previously described.[54]

Cryogenic transmission electron microscopy (cryo-TEM)

Suspensions of the LNPs were added to Quantifoil Cu1.2/1.3 grids, and frozen in liquid ethane using FEI Vitrobot MarkIV. The grids were stored in liquid nitrogen until used for imaging. JEM-2200FS (JEOL, Japan) was used to obtain the images. The instrument was operated at 200 kV. A DE-20 camera was used to capture images. Samples were imaged at a 30,000× magnification. Sample preparation and imaging was performed by Terabase Inc. (Aichi, Japan).

Animals

The experimental protocols were all reviewed and approved by the Hokkaido University Animal Care Committee under the guidelines for the care and use of laboratory animals. BALB/c mice (female, 4 weeks old) and C.KOR/Stm Slc-Apoe mice (female, 4 weeks old) were sourced from Japan SLC (Shizuoka, Japan). Mice were maintained on a regular 12-h light/12-h dark cycle in a specific animal facility at Hokkaido University. Four to five mice were housed in each cage. The mice were fed a pelleted mouse diet (cat# 5053, LabDiet, USA) and were provided water *ad libitum*.

Measurement of Fluc activity

Mice were intravenously injected with Fluc mRNA-loaded LNPs at a dose of 0.01 mg mRNA/kg. Six hours after the injection, the mice were euthanized. Tissue was then collected, frozen in liquid nitrogen, and stored at −80°C. All tissue was homogenized in a passive lysis buffer (Promega, Madison, WI, USA) using Micro Smash MS-100R (TOMY Seiko Co., Ltd., Tokyo, Japan). Debris was removed via centrifugation. Fluc activity in the supernatant was measured using the Luciferase Assay System (Promega) according to the manufacturer's protocol. Luminescence was measured using a luminometer (Luminescencer-PSN, ATTO, Japan). Protein concentrations were determined using a BCA Protein Assay Kit (Pierce, Rockford, IL, USA). Fluc activity was expressed as relative light units (RLU) per mg of protein.

Measurement of serum TTR protein levels

Mice were intravenously injected with Cas9/sgTTR RNP-loaded LNPs at the indicated dose. The mice were euthanized at the indicated time point after injection, and blood was collected, clotted at room temperature for 1 h, and serum was isolated by centrifugation (25°C, 1,000×g, 15 min). The TTR protein concentration in serum was determined using a Prealbumin ELISA Kit (mouse) (Aviva Systems Biology, CA, USA) according to the manufacturer's protocol.

Genomic analysis

Mice were intravenously injected with Cas9/sgTTR RNP-loaded LNPs at a dose of 2 mg RNP/kg. The mice were euthanized 3 months after injection, and liver tissue was collected. DNA was extracted and purified from the liver and spleen using NucleoSpin Tissue (Takara Bio, Japan). Next-generation sequencing was performed by the Bioengineering Lab. Co., Ltd. (Kanagawa, Japan). Briefly, the purified DNA was amplified using a two-step tailed PCR, and sequencing was performed using an Illumina MiSeq instrument in the paired-end mode. The primers for the TTR locus were as follows: forward 5′-TCG TCG GCA GCG TCA GAT GTG TAT AAG AGA CAG GCT TTG GAA ACA ATG CTG TCT AT-3′ and reverse 5′-GTC TCG TGG GCT CGG AGA TGT GTA TAA GAG ACA GTG GGC TTT CTA CAA GCT TAC C-3′. The genome editing outcomes were analyzed using CRISPResso2.

Measurement of plasma F9 activity

Mice were intravenously injected with Cas9/sgF9 RNP-loaded LNPs at a dose of 2 mg RNP/kg. The mice were euthanized at the indicated time points after injection. Blood was collected and mixed with 3.21% sodium citrate (pH5.5) at a volume ratio of 9:1, and the plasma was isolated via centrifugation (4°C, 2,500×g, 15 min). The F9 activity in plasma was determined using the Revohem FIX Chromogenic Measurement Kit (Sysmex Corporation, Hyogo, Japan) according to the manufacturer's protocol.

Measurement of plasma antithrombin (AT) protein levels

Mice were intravenously injected with Cas9/sgAT RNP-loaded LNPs at a dose of 1.5 mg RNP/kg. The mice were euthanized at 7 days after injection. The blood was collected, treated with heparin, and the plasma was isolated via centrifugation (4°C, 3,000×g, 5 min). The AT protein level in the plasma was determined using a Mouse Antithrombin III ELISA Kit (SERPINC1) (Abcam, Cambridge, England) according to the manufacturer's protocol.

Quantification of ionizable lipids in tissues

Mice were intravenously injected with RNP-loaded LNPs at a dose of 2 mg RNP/kg. The mice were euthanized at the indicated time points after injection, and each liver and spleen was collected. At the same time, blood was collected, treated with heparin, and plasma was isolated by centrifugation (4°C, 1,000×g, 15 min). All samples were stored at −80°C before analysis for lipid quantification by liquid chromatography-mass spectrometry (LC/MS). All tissue was homogenized in 400 μL of water. The tissue homogenates (50 μL) were extracted with 400 μL of acetonitrile/isopropanol (v/v 50:50). After centrifugation (4°C, 15,000×g, 10 min), the supernatant was filtered, and the filtrate was transferred to a vial for LC/MS analysis. The samples were analyzed using the Nexera lite system (Shimadzu Corporation, Kyoto, Japan) equipped with a Shim-pack Arata C18 (2.0 × 50 mm, 5 μm) with a gradient mobile phase of water (5 mM ammonium acetate) and acetonitrile/isopropanol (v/v 1:2) (5 mM ammonium acetate) at 60°C with a flow rate of 0.2 mL/min for 15 min. The samples were detected using an LCMS-2050 (Shimadzu Corporation) under optimized conditions for the detection of ionizable lipids and their degraded products, monoacylated alkanolamines, in the positive ion mode. Each of the molecules were monitored using masses of $[M + H]^+ \rightarrow$ 780.7 (CL4F11_ζ-2), 864.8 (CL4F6), 916.9 (CL4H6), 584.6 (monoacylated alkanolamine from CL4F11_ζ-2), and 652.6 (monoacylated alkanolamine from CL4H6).

Single-dose toxicity test

Mice were intravenously injected with the RNP-loaded ζ-LNPs at a dose of 2 mg RNP/kg. Seven days after the injection, the mice were anesthetized. For serum chemistry examinations, blood was obtained via the inferior vena cava and processed to serum. Serum chemistry parameters were measured at the Oriental yeast Co., Ltd. (Shiga, Japan). For histopathological examination, the liver and spleen were collected and fixed in Mildform 10N. Three μm slices were stained with Hematoxylin-Eosin, and were observed and evaluated at the Sapporo General Pathology Laboratory Co., Ltd. (Hokkaido, Japan).

Evaluation of biodistribution

Mice were intravenously injected with 0.5% DiR-labeled LNPs at a dose of 0.75 mg RNP/kg. The dosage of siRNA-loaded LNPs was consistent with the lipid doses of the RNP-loaded LNPs. Blood and tissues were isolated 1 h after injection. The fluorescence intensity was measured using an *in vivo* imaging system, 200 series (PerkinElmer, US).

In vitro cellular uptake study

Hepa1c1c7 cells were maintained in PRMI-1640 supplemented with 10% FBS at 37°C in 5% CO_2. Hepa1c1c7 cells were seeded at 2×10^4 cells per well in 24-well plates in growth media 24 h prior to transfection. The 0.002 mol % DiD-labeled LNPs were diluted either with RPMI-1640 or that containing 10% FBS, 3 μg/mL hrApoE3 protein, 30 mg/mL BSA, or both hrApoE3 protein and BSA to reach lipid concentrations of 100 μM, which was followed by incubation for 15 min at 37°C. The diluted LNPs were then added to the cells following the aspiration of spent media. Following 1 h of incubation at 37°C in 5% CO_2, the cells were washed twice with PBS(−) containing 20 U/mL heparin at the indicated times and collected by trypsin treatment. The cells were centrifuged and, after removing the supernatant, were resuspended with FACS buffer (PBS(−) containing 0.5% bovine serum albumin and 0.02% sodium azide). The cells were filtered through a nylon mesh and measured using a CytoFLEX Flow Cytometer (Beckman Coulter, Inc., CA, USA).

Analysis of protein corona

The LNPs were mixed with freshly isolated mouse EDTA-plasma. After incubation for 1 h at 37°C, the protein-bound LNPs were purified by size exclusion chromatography followed by ultracentrifugation. PBS(−) mixed with the plasma (without LNPs) was used as a negative control to expose the amount of contaminated LNP-unbound proteins. The isolated LNP-bound proteins were extracted to remove lipids via the use of a ReadyPrep 2-D Cleanup Kit (Bio-Rad Laboratories, Inc., CA, USA) according to the manufacturer's protocol. The concentration of the purified proteins was measured using a CBQCA Protein Quantitation Kit (Thermo Fisher Scientific) according to the manufacturer's protocol. Proteome analysis using a nanoLC-MS/MS was performed at Promega.

QUANTIFICATION AND STATISTICAL ANALYSIS

Results are expressed as the mean ± the SD used in independent experiments. *p* values were calculated using a Student's t test and one-way analysis of variance (ANOVA) with appropriate *post hoc* testing as indicated in the figure legends. Group size, definition of center, and dispersion and precision measures are also noted in the figure legends as appropriate. All statistics were completed using GraphPad Prism software version 10.1.2 (San Diego, CA, USA).